Published in final edited form as:
J Comp Neurol. 2013 June 1; 521(8): 1844–1866. doi:10.1002/cne.23263.

Hypothalamic and Other Connections with the Dorsal CA2 Area of the Mouse Hippocampus

Zhenzhong Cui[1], **Charles R. Gerfen**[2], and **W. Scott Young 3rd**[1]

[1]Section on Neural Gene Expression, National Institute of Mental Health, National Institutes of Health, Department of Health and Human Services, Bethesda, Maryland 20892

[2]Laboratory of Systems Neuroscience, National Institute of Mental Health, National Institutes of Health, Department of Health and Human Services, Bethesda, Maryland 20892

Abstract

The CA2 area is an important, although relatively unexplored, component of the hippocampus. We used various tracers to provide a comprehensive analysis of CA2 connections in C57BL/6J mice. Using various adeno-associated viruses that express fluorescent proteins, we found a vasopressinergic projection from the paraventricular nuclei of the hypothalamus (PVN) to the CA2, as well as a projection from pyramidal neurons of the CA2 to the supramammillary nuclei. These projections were confirmed by retrograde tracing. As expected, we observed CA2 afferent projections from neurons in ipsilateral entorhinal cortical layer II as well as from bilateral dorsal CA2 and CA3 using retrograde tracers. Additionally, we saw CA2 neuronal input from bilateral medial septal nuclei, vertical and horizontal limbs of the nucleus of diagonal band of Broca, supramammillary nuclei (SUM) and median raphe nucleus. Dorsal CA2 injections of adeno-associated virus expressing green fluorescent protein revealed axonal projections primarily to dorsal CA1, CA2 and CA3 bilaterally. No projection was detected to the entorhinal cortex from the dorsal CA2. These results are consistent with recent observations that the dorsal CA2 forms disynaptic connections with the entorhinal cortex to influence dynamic memory processing. Mouse dorsal CA2 neurons send bilateral projections to the medial and lateral septal nuclei, vertical and horizontal limbs of the diagonal band of Broca and the SUM. Novel connections from the PVN and to the SUM suggest important regulatory roles for CA2 in mediating social and emotional input for memory processing.

Keywords

hippocampal CA2; entorhinal cortex; paraventricular nucleus; supramammillary nucleus; median raphe nucleus; septum; anterograde tracer; Fluorogold; Green Beads; AAV-GFP; AAV-tdTomato; cre recombinase; adeno-associated virus; vasopressin

Correspondence: W. Scott Young, National Institute of Mental Health, NIH, 9000 Rockville Pike, MSC 4483, Building 49, Room 5A56, Bethesda, MD 20892-4483, TEL: 301-496-8767, FAX: 301-402-6473, wsy@mail.nih.gov.

Conflict of interest statement

No known conflicts of interest.

Roles of authors

All authors listed on the paper must have contributed significantly to the elaboration of the paper and/or to the research that led to preparation of the manuscript:

All authors had full access to all the data in the study and take responsibility for the integrity of the data and the accuracy of the data analysis. Study concept and design: ZC, WSY. Acquisition of data: ZC, CRG. Analysis and interpretation of data: ZC, CRG, WSY. Drafting of the manuscript: ZC, WSY. Critical revision of the manuscript for important intellectual content: ZC, CRG, WSY. Study supervision: WSY.

Introduction

Although 75 years have passed since Lorente de Nó first defined the small, transitional CA2 zone as a distinct hippocampal region based on the properties of its pyramidal neurons and described in mouse and monkey some fibers systems in regard to CA2 (Lorente., 1934), its precise functions are still largely unexplained (Chevaleyre and Siegelbaum, 2010). Signals from the entorhinal cortex travel through the perforant path in a unidirectional pathway to the dentate gyrus. Continuing this feed-forward tri-synaptic excitatory circuit, the dentate gyrus projects via mossy fibers to CA3, which in turn projects via Schaffer collateral axons to CA1 (Andersen, 2007; van Strien et al., 2009). This pathway omits the CA2.

Recent work suggests the CA2 is a distinct hippocampal zone that participates in hippocampal function and has a role in learning and memory. For example, the use of specific molecular markers allowed researchers to define CA2 and its boundaries (Lein et al., 2005b; Zhao et al., 2001). These results support the claim for CA2 as a separate hippocampal zone (Thompson et al., 2008) with at least 50 genes discretely expressed in CA2 pyramidal cells or interneurons (Lein et al., 2005b; Lein et al., 2007; Zhao et al., 2001). In this regard, the Trek1 gene (Kcnk2), which is associated with resistance to depression (Liou et al., 2009; Perlis et al., 2008), is highly expressed in CA2 (Talley et al., 2001). FGF2, enriched in the CA2 (Turner et al., 2011), is expressed at lower levels in the hippocampus of patients with major depressive disorder (Evans et al., 2004; Gaughran et al., 2006).

CA2 non-pyramidal neurons are less numerous in the brains of schizophrenic and manic-depressive patients (Benes et al., 1998). CA2 neurons are also resistant to damage from some forms of disease, including epilepsy (Brierley and Graham, 1984; Dam, 1980; Honkaniemi and Sharp, 1999; Meldrum and Corsellis, 1984; Sperk, 1994; Williamson and Spencer, 1994). Electrophysiological studies indicate that CA2 neurons uniquely lack typical long-term potentiation (LTP) and more current is required for action potential activation (Zhao et al., 2007). CA2 neurons demonstrate much greater response to distal than proximal dendritic excitation from the entorhinal cortex (Chevaleyre and Siegelbaum, 2010). The adenosine A1 receptor enables caffeine to induce synaptic potentiation in CA2 neurons (Simons et al., 2012).

Recent work suggests that the CA2 region plays a functional role in memory. The vasopressin 1b receptor (Avpr1b) mRNA is predominantly expressed in dorsal CA2 pyramidal neurons (Young et al., 2006), and Avpr1b knockout (KO) mice exhibit reduced social recognition and social aggression (Wersinger et al., 2007; Wersinger et al., 2002; Wersinger et al., 2008). Electrophysiological studies have shown that vasopressin permits synaptic potentiation in hippocampal CA2 neurons (Zhao et al., 2010). Behavioral tests, moreover, show that Avpr1b KO mice have impaired memory for temporal order that is believed to be hippocampally dependent (DeVito et al., 2009). We previously hypothesized that the Avpr1b in CA2 permits coupling of social context with an experience (Young et al., 2006).

Our current understanding of dorsal CA2's connectivity has gaps about how it might fulfill unique functional roles. The current study was designed to help elucidate an integrated role for the dorsal CA2 in hippocampal circuitry in mice by using retrograde and AAV-expressing anterograde fluorescent tracers to comprehensively study its afferents and efferents, respectively. We confirm numerous CA2 connections previously described in other species as well as novel afferent and efferent connections from the hypothalamic paraventricular nucleus (PVN) and to the supramammillary area (SUM), respectively.

Materials and Methods

Animals

A total of 46 male mice between 80–90 days old (22–25g) were used for this study. Twenty-one C57BL/6J mice (Jackson Labs, Bar Harbor, ME) were used for retrograde tracer injections. Seventeen mice received fluorogold (Fluorochrome, LLC, Denver, CO) injections: fourteen in CA2; and as controls, one in CA1 and two in the cortex dorsal to the CA2. Four mice received green Retrobeads (LumaFluor, Inc., Durham, NC) injected into dorsal CA2 (henceforth, any referral to hippocampal injections or projections in this study refer to the dorsal hippocampus unless specifically mentioned otherwise). Eighteen mice were used for AAV-GFP injections. Eight mice received injections either unilaterally or bilaterally into CA2. Ten mice received unilateral injections of AAV-GFP into the PVN. In addition, three transgenic mice that express Cre within vasopressin (Avp) neurons of the PVN (GENSAT line number QZ27) were injected unilaterally with AAV-tdTomato in the PVN. This enables a red fluorescent protein to be expressed in those cells that express Cre; in this case, in the vasopressinergic neurons of the PVN. Finally, another 4 male mice were used for fluorogold retrograde labeling studies to examine the CA2 projection to the SUM.

All mice were maintained on a 12-hour light/dark cycle (lights on at 4:00 AM) with food and water available ad libitum. All animal procedures were approved by the National Institute of Mental Health Animal Care and Use Committee and were in accordance with the National Institutes of Health guidelines on the care and use of animals.

Tracers and Virus

Fluorogold was dissolved at 4% in normal saline, 1% in normal saline or 1% in 0.2M sodium cacodylate buffer, pH 7.4, and injected in mice to evaluate different concentrations and formulations for optimizing detection with minimal spread outside CA2. Green Retrobeads were injected in the original solution. All aliquots were stored in refrigerated dark boxes. AAV-GFP (AAV2/6 CMV.PI.EGFP.WPRE.bGH) was obtained either as a gift from Dr. Harold Gainer (NINDS, NIH) or purchased from University of Pennsylvania Vector Core, Philadelphia, PA (stock number CS0026) with titers of about $10^{11–12}$ infectious particles/ml. AAV-tdTomato (AAV2/9.CAG.FLEX.tdTomato-WPRE.bGH(Allen 864), lot number V1682) was also obtained from the Vector Core at about the same titer.

Surgical procedures

Mice were anesthetized with 250–500 mg/kg i.p. injections of tribromoethanol (Avertin) and kept warm with a heating pad while under anesthesia and while recovering. During surgery, the mouse was placed in a small animal stereotaxic instrument (Benchmark Angle Two, Leica), an ophthalmic ointment was applied to prevent drying of the eyes, skull hair was plucked, the area was disinfected, and a small incision was made to expose the skull. The skull was then opened over the appropriate stereotaxic coordinates using a small burr (0.45mm) drill. A blunt-end needle was used for the injection. Following needle removal, the skin was closed with wound clips. The mouse received 0.35 ml of warm saline i.p. and was observed until awake. The mouse was then returned to its home cage and monitored carefully for the first 48 hours. Surgery was conducted in accordance with NIH Guidelines for rodent survival surgery.

Tracer Injections

Each mouse received a single pressure injection of retrograde tracer using a Hamilton syringe with a 33 gauge blunt-end needle mounted on a stereotaxic device. Injections targeted one of two CA2 areas in the dorsal hippocampus: dorsomedial (site 1) at medial-lateral (ML) relative to midline: 0.80 mm; anterior-posterior (AP) relative to bregma: −1.06

mm; and dorsal-ventral (DV) relative to surface of the brain: −1.76 mm or a dorsolateral (site 2) at ML: 1.85; AP: −1.70; DV: −1.85 mm (subsequent coordinates reported in same order, i.e., ML, AP, DV). Fluorogold injections were given at one of three doses: 30nl (three mice), 20nl (seven mice), or 10nl (six mice). The latter volume provided the most localized CA2 targeting (least spread to adjacent areas). Green Retrobeads were administered in doses of 120nl per injection. To reduce leakage through the needle, 5nl of mineral oil was backfilled into the needle before and after the 10nl of fluorogold tracer, making the total injection volume 20nl. For SUM injections, 50nl of 1% fluorogold were injected there unilaterally at ML: 0.40, AP: −2.80, DV: −4.85 mm. Injection speed for fluorogold was 1nl/min (except 5nl/min for the SUM injections) and for green Retrobeads 10nl/min.

AAV-GFP Injections

Recombinant AAV-GFP was delivered by pressure injection through a 30 gauge, blunt-end needle Hamilton syringe in eight mice for dorsal CA2 injections. 400 nl were injected into each injection site in the dorsal CA2 at either 2 (0.8μl total) or 6 (2.4μl total) sites. For two-point injections, the unilateral coordinates (ML, AP, DV) were 0.80, −1.06, −1.76 mm and 1.90, −1.70, −1.80 mm. Six-point injections were performed bilaterally (three on each side) to cover extensively the dorsal CA2 of six mice. Injections were made at: −1.25, −1.22, −1.73 mm; 1.25, −1.22, −1.73 mm; −2.00, −1.70, −1.83 mm; 2.00, −1.70, −1.83 mm; −2.60, −2.18, −2.15 mm; and 2.60, −2.18, −2.15mm. For PVN injections, 200nl of AAV-GFP were injected at either 0.22, −0.82, −4.90 mm or 0.22, −0.94, −4.90 mm in six mice. In four mice, the PVN was approached at either 20° or 40° off vertical. The syringe was backfilled with 5nl of mineral oil prior to loading AAV virus to reduce leakage. Injection speed was 10–20nl/min.

AAV-tdTomato Injections

Similar to the AAV-GFP injections, Cre-activated AAV-tdTomato was injected unilaterally to the PVN area of the Avp Cre transgenic mice. Thirty nl of AAV-tdTomato were injected at 0.22, −0.94, −4.90 mm. The syringe was backfilled with 5 nl of mineral oil prior to loading AAV virus to reduce leakage. Injection speed was 5 nl/min.

Perfusion of the injected brains

Seven to ten days (or 28 days for the cacodylate-buffered fluorogold per observations for transport to the PVN in the rat (Zhang and Hernandez, 2011)) after retrograde tracer injections, mice were deeply anesthetized with isoflurane and perfused transcardially with 10ml of ice-cold normal saline followed by 30ml of ice-cold 4% paraformaldehyde (PFA) solution. To prepare most brains for cryo-sectioning, the brains were fixed overnight in 4% PFA solution followed by 20% of sucrose in normal saline overnight. Cryostat sections 16 μm thick were collected from the entire brain and mounted onto SuperFrost Plus slides (Fisher, Waltham, MA) consecutively. A few mice that received cacodylate-buffered fluorogold injections were perfused with 4% PFA and fixed overnight in 4% PFA before transfer to a phosphate-buffered saline solution for sectioning on a microtome at 30 μm; the entire brain was cut and sections were mounted on the slides. Slides were stored in light-proof boxes.

DAPI staining

4′–6-Diamidino-2-phenylindole (DAPI) forms fluorescent complexes with double-stranded DNA to stain nuclei. Some sections on the slides were submerged in the DAPI solution (1:25,000 dilution of stock solution, D1036; Life Technologies, Carlsbad, CA) for 1–3 minutes followed by PBS rinsing.

Image Processing

The images were taken by adding one or two drops of saline with cover glass. Images were acquired using a fluorescent microscope (Nikon 50i) with a DAPI filter for Fluorogold and DAPI stained sections, a FITC filter for green Retrobeads and GFP, and DsRed filter for tdTomato fluorescence. iVision (BioVision Technologies, Exton, PA) was used to process images with exposure times set, depending on signal intensity, between 800–6000 milliseconds. A few images had their contrast or brightness slightly enhanced.

Results

Unilateral injections of retrograde tracers into the dorsal hippocampal CA2 region

Afferent projections to the dorsal hippocampal CA2 region were analyzed with injections of the retrograde tracers, fluorogold and green Retrobeads. Typical injection sites are shown in Figure 1. Fluorogold injections were made into the dorsomedial CA2 (Fig. 1A,F) or dorsolateral CA2 region (Fig. 1B). The injection sites were identified in Nissl stained sections (C,D) and fluorogold staining in the surrounding neuropil provides an estimate of the spread of the tracer. The distribution of labeled neurons at the injection site provides a rough estimate of the spread of the tracer, but does not definitively demarcate the area from which tracer is taken up. In some injections there is evidence of leakage along the needle injection tract as seen in the cortical areas above the hippocampal injection target (Fig 1F). To control for such spread, control injections limited to the cortex were made. (data not shown). Green Retrobeads were injected in the dorsolateral CA2 region (Fig. 1E). Due to the relatively poorer neuronal labeling by green Retrobeads, fluorogold was used more often.

CA2 afferent projections from the entorhinal cortex

As shown in Fig. 2, our tracer results revealed that most of the cortical input to CA2 originates in layer II of the ipsilateral medial and lateral entorhinal cortices (MEC, LEC), presumably through the perforant pathway. The dorsal two thirds of LEC and MEC layer II neurons send their projections to dorsal CA2 as revealed by either dorsolateral CA2 (Fig. 2A–D,G) or dorsomedial (Fig. 2F) injections. Green Retrobeads were also retrogradely transported to the entorhinal cortex layer II neurons (Fig. 1E for injection, Fig. 2E for LEC labeling). Fewer, less intensely labeled neurons in layer III were labeled (Fig. 2G). We did not observe projections to dorsal CA2 from the ventral third of either MEC or LEC. We did see much lower labeling of the contralateral MEC and LEC. No projections from the amygdala were observed.

Intrahippocampal CA2 afferent projections

CA2 receives a projection from ipsilateral CA3 neurons (Fig. 1A,B,3D). A slight spread of the injection to the CA3 region seems unlikely as we did not see retrograde labeling within the dentate gyrus via its heavy mossy fiber projection to CA3. Abundant CA2 afferent projections from the contralateral CA3 and CA2 were revealed after unilateral CA2 fluorogold injections either in the dorsomedial (Fig. 3A,B) or dorsolateral CA2 (Fig. 3C,D). No neuronal projections from region CA1 to CA2 were ever spotted in this retrograde tracer study. Although topographical features may presumably exist for CA2 projections, they were not studied here.

CA2 afferent projections from the septal nuclei and nuclei of the diagonal bands of Broca

Labeling in the medial septal nucleus was clearly and repeatedly observed, with perhaps more labeling in the ipsilateral MS (Fig. 4A). Only a few scattered labeled cells were detectable in the lateral septal nuclei in some of the CA2 injected mice and no consistent

pattern was seen (data was not shown). Bilateral neuronal projections from both the vertical and horizontal limbs of the diagonal bands of Broca were seen (Fig. 4B).

CA2 afferent projections from the PVN

Although vasopressin 1b receptor (Avpr1b) mRNA is almost exclusively expressed in dorsal CA2 pyramidal neurons in mouse brain (Young et al., 2006), to date no afferent projections from the Avp-containing neurons of the PVN have been reported. To re-examine this pathway with retrograde tracing methods, we injected fluorogold into the CA2 region and allowed a survival period of either 1 or 4 weeks. Following a one week survival, there was no evidence of retrogradely labeled cells in the PVN. However, with a 4 week survival period (N=3), CA2 injections(Fig. 5A,C) led to retrograde labeling of neurons in the PVN (Fig. 5B,D). To control for the possibility that the longer time expanded the area from which tracer was taken up, injections were made into the CA1 region. Following a 4 week survival, there was no evidence of retrograde labeling of PVN neurons (Fig. 5E,F).

CA2 afferent projections from the PVN confirmed using fluorescent protein-expressing AAV injections

We performed unilateral AAV-GFP injections (200nl) into the PVN and surrounding region (Fig. 6A,B). We observed GFP in fibers surrounding the pyramidal cells of the CA2 bilaterally, as well as in the immediately adjacent CA3 (Fig. 6C,D,E). DAPI staining revealed that the GFP-positive axonal fibers presumably originating from the PVN targeted CA2 and immediately adjacent CA3 (Fig. 6E). We also observed GFP-positive fibers with the fornix anterior to the injection site but not posterior to it suggesting that the PVN projects to the CA2 through the fornix (Fig. 6F).

We were concerned that leakage of AAV-GFP along the needle track might infect other neurons (or fiber pathways). We never found labeled neurons within the hippocampus from the vertical track to the PVN injections. However, to be cautious, we also chose 2 other approach angles. Both 20° and 40° tracks off vertical resulted in similar patterns of labeling within the PVN and CA2 (data not shown).

CA2 afferent projections from the PVN are, in part, vasopressinergic

To determine if the neurons in the PVN that project to the CA2 are, at least in part, vasopressinergic we made use of a transgenic mouse line that expresses Cre within Avp neurons (GENSAT line QZ27; Fig. 7A). We injected AAV that expresses tdTomato in the presence of Cre into the PVN. In this situation, only the Avp neurons of the PVN would be labeled (there are no non-PVN neurons that express Avp in the vicinity of the injection). Three weeks after the AAV-tdTomato injection, a group of neurons within the PVN were labeled (Fig. 7B). The majority of the labeled cells appear to be magnocellular neurons; however, a few smaller neurons were also visible. Both dorsomedial and dorsolateral CA2 and immediately adjacent CA3 had fluorescent fibers primarily within the pyramidal cell layer (Fig. 7C). As in the examples above, the PVN to CA2 vasopressinergic projections are bilateral. Faint, fine fluorescent fibers were also detectable within the fimbria (Fig. 7D).

CA2 afferent projections from the supramammillary nucleus

Groups of SUM neurons located near (above) the mammillothalamic track were labeled after injection of retrograde tracer into either CA2 site (dorsomedial or dorsolateral). Typical labeling patterns are shown in coronal (Fig. 4C) and horizontal (Fig. 4E) sections. We observed this labeling in all four correctly targeted mice.

Other subcortical CA2 afferent projections

Most, though not all, CA2 injections labeled the median raphe nucleus (see Fig. 4D,F). There was no clear labeling of noradrenergic neurons in the locus coeruleus or in the dopaminergic neurons of the ventral tegmental area. A few labeled neurons were seen in substantia nigra (pars reticulata) for some of CA2 injected mice, but the pattern was not consistent (data not shown).

Technical considerations for retrograde tracer studies

We found that it was possible to inject as little as 10nl of fluorogold (either 1% or 4%) in order to target CA2 neurons precisely. Because the pressure injection method always produced a small amount of leakage through needle track, we did identical neocortical injections above the CA2 as a control (data not shown). In these mice, we observed labeling only in certain groups of thalamic neurons in the ventral posteromedial thalamus nucleus. Similar patterns of thalamic labeling, although much weaker, occurred in the CA2-injected group and as there are no reports of neuronal input from thalamus to CA2, we believe that the retrograde thalamic labeling observed following CA2 area injections was due to the cortical leakage and resultant labeling of known thalamocortical projections to the sensorimotor cortex.

Another technical consideration is the advantage of the small amount (10nl) of retrograde tracer injected. This amount allowed us to avoid spillover to the CA3 and subsequent retrograde labeling of the dentate gyrus granule cells via the mossy fibers with the fluorogold injections. Results presented above were from mice with precise targeting and no dentate gyrus labeling. The small injections amounts, however, also generally led to lighter staining. Subcortical projecting neurons tended to be less intensely labeled compared to those in layer II of the entorhinal cortices or in the hippocampus.

Finally, it is curious that we saw no intrahippocampal retrograde transport from CA2 to CA3 using green Retrobeads (Fig. 1E) unlike with Fluorogold (e.g., Fig. 1B). The green Retrobeads only label a subset of the fibers (e.g., from entorhinal cortex, median raphe) that are defined by fluorogold and AAV-GFP tracing. Fiber-type selective failure of retrograde transport has been observed previously with green Retrobeads (Deng and Rogers, 1999).

Intrahippocampal CA2 efferent projections

We made unilateral pairs of AAV-GFP injections in the dorsomedial and dorsolateral CA2 (Fig. 8A,B) to study CA2 efferent projections. We also accurately made injections in three sites bilaterally of AAV-GFP in two mice to provide a more comprehensive picture of the dorsal CA2 efferent projections (Fig. 10). In comparison with the unilateral two-site injected mice, these six-site injected mice displayed essentially identical projection patterns, but with more intensity at the axonal targets (compare Figs. 8–9 to 10–12). Both the ipsilateral and contralateral intrahippocampal projections to CA1, CA2, and CA3 are labeled (Fig. 8B,E,F,H). Within CA1 bilaterally, fluorescence is more intense in the stratum oriens (especially adjacent to the pyramidal cell layer) compared to the strata radiatum and lacunosum moleculare (Fig. 8B,F,H; Fig. 10A–C,G–I; Fig. 11A–F,G, H,N). With unilateral injections we saw little or no labeling in the contralateral CA2 stratum lacunosum moleculare. This labeling in stratum oriens fades across CA2 to CA3 while stratum radiatum fluorescence becomes somewhat higher going to CA3. Except within the injection site and immediately adjacent in CA3, fibers were infrequent in the pyramidal cell layer (Fig. 8B,F,H; Fig. 10A–C,G–I; Fig. 11A–F,G, H,N). Ventral portions of the hippocampus in general showed much less or no fluorescence (data not shown). Fibers connecting the hippocampi were prominent in the dorsal hippocampal commissure (Fig. 8G; Fig. 11L). GFP-positive fibers were prominent in the fimbria (Fig. 11M). The subiculum as well as

overlying cortex do not receive CA2 neuronal projections (Fig. 11E–F). The entire entorhinal cortex and amygdala are also devoid of CA2 efferent projections (data not shown).

CA2 efferent projections to the septal nuclei and nuclei of the diagonal bands of Broca

The dorsal CA2 also sends projections to the MS and LSD, as well as the VDB and HDB (Fig. 9, 12). The projections to the septal nuclei, VDB and HDB most likely course through the fornix where labeled fibers were plentiful (Fig. 12B,C).

CA2 efferent projections to the supramammillary nucleus

A novel projection from CA2 to the supramammillary nucleus (SUM) was identified in cases of AAV-GFP injections into the hippocampus. In cases of bilateral injections into the CA2 region at 3 sites along the rostro-caudal axis, labeled fibers extend from the fornix into the SUM nucleus. Labeled axons with terminals distributed throughout most of the SUM and no labeling was evident in the mammillary nucleus. These cases with bilateral injections totaling 6 injections, may be expected to label most of the CA2 projection to the SUM. Cases of single injections into the CA2 into one side labeled axonal fibers and terminals that were more restricted in their distribution with more prominent labeling into the lateral part of the nucleus (Fig. 13A,B). This suggests there may be some topographic organization in these projections. The unilateral injections did provide bilateral projections to the SUM. In each of the injections, neurons labeled at the injection site appeared to be localized primarily to the CA2 hippocampal field, although there may have been involvement of some adjacent CA1 and CA3 neurons.

To confirm the CA2 to SUM projection we injected fluorogold into the SUM (Fig 13C,F). The injection sites appeared to cover the SUM, with no apparent spread into the mammillary nuclei. Retrogradely labeled neurons were observed in the CA2 hippocampal field, although there may have been a few neurons present in the adjacent CA3 field as well. Retrogradely labeled hippocampal neurons displayed radially oriented dendrites indicating that they were pyramidal principal neurons (Fig. 13D,E,G). As expected from the anterograde tracing cases, retrogradely labeled neurons were present in the CA2 field bilaterally.

Other investigated areas

Other than the aforementioned brain areas, no noticeable GFP-positive fibers were seen in other brain regions. In particular, no labeled fibers were seen in the MEC, LEC, other cortical regions, amygdala, thalamus, PVN, ventral tegmental area, substantia nigra, raphe nuclei, or locus coeruleus (LC).

Discussion

In this study we examined the connections of the CA2 region of the hippocampus in the mouse using AAV-expression vectors and fluorescent retrograde tracing techniques. Using these techniques we identified a novel afferent projection from the hypothalamic PVN vasopressin neurons to CA2 and a novel efferent projection from CA2 to the supramammillary nucleus. We also observed afferent connections to CA2 from the medial and lateral entorhinal cortices, bilateral CA2 and CA3, medial septum, ventral and horizontal diagonal bands of Broca, supramammillary nuclei and median raphe. These latter two sites, we believe, had not been confirmed by retrograde tracing previously. Efferent connections were shown from CA2 to the CA1, CA2, CA3, medial septum, dorsal part of the lateral septum, triangular septal nucleus, and ventral and horizontal diagonal bands of Broca. As discussed below, many of these connections have been described previously in

rats and monkeys, primarily, and may be viewed in the context of known hippocampal functional circuits.

Although connections of the PVN, SUM and CA2 hippocampal region have been extensively studied, the present finding of CA2 afferents from the PVN and efferents to the SUM are novel. This is most likely attributed to increased sensitivity of the axonal tracing methods used. In the case of retrograde labeling of CA2 afferents from the PVN, the longer survival time required attests to the difficulty of labeling this pathway. In such cases it is necessary to assure that labeling is not due to uptake into other pathways. Controls for such a possibility were provided by injections into adjacent brain regions. Additionally, the concordance of complementary anterograde and retrograde axonal tracing methods to label the pathways from the neurons of origin in the PVN to CA2provide further evidence for the existence of the pathway reported. In particular, labeling produced with an AAV-Cre dependent expression vector produced very selective labeling of PVN neurons and their axonal projections. Together, results produced with the use of multiple axonal tracing methods provide definitive evidence of PVN axonal projections to the CA2 (and immediately adjacent CA3) hippocampus. Similar concordant results were also obtained using anterograde and retrograde axonal tracing methods to demonstrate axonal projections from the CA2 to the SUM.

Other technical concerns that were considered in our analysis included the question of possible uptake of fluorogold by fibers of passage. Evidence exists that it can be taken up by fibers of passage, at least in some sites (Leak and Moore, 1997). Thus, the importance of anterograde confirmation and whether uptake by fibers of passage or axon terminals could lead to AAV-mediated GFP expression (this is not a concern with the tdTomato tracer as it is is only activated by Cre expressed within the vasopressin neurons of the PVN so other sites of uptake and transport of virus are invisible). Some studies find essentially no fibers-of-passage uptake (Chamberlin et al., 1998; Klein et al., 1998) while others the opposite (Alisky et al., 2000; Kaspar et al., 2002). In this study, we saw no evidence for retrograde transport, either from fibers of passage or axon terminals in the hippocampus. If we had, the cell bodies of those axons would have had to express GFP as the AAV works through integration into the nuclear genome. For example, we saw no GFP-positive cell bodies in the entorhinal cortex or contralateral hippocampus after unilateral hippocampal injections (e.g., Fig. 8). Similarly, only a very few CA3 neurons adjacent to the well-targeted injection sites were labeled with GFP indicating that fibers of passage from ipsilateral injections were not labeling CA3 neurons outside the injection site. Therefore, that specificity of anterograde tracing in combination with the retrograde tracing enables us to be confident in our interpretations.

Another important technical concern is the accuracy of our injections and that depends to an extent on the determination of CA2 boundaries. We first became interested in the CA2 when we studied where the Avpr1b was expressed in mice (Young et al., 2006). At that time, we were guided by the boundaries of the expressions of various genes as demonstrated by Lein and coworkers (Lein et al., 2005a; Lein et al., 2004). As is evident from their cell stains in Figs. 1J and 4F (Lein et al., 2005a), Fig. 2 from our Avpr1b paper (Young et al., 2006) and Fig. 1D in this paper, the boundaries are relatively apparent in the dorsolateral hippocampal CA2. Progressing from CA1 to CA2, the cell density in the pyramidal cell layer abruptly decreases and when progressing from CA2 to CA3, the thickness in that layer subtly increases. This knowledge combined with accurately placed, small-sized injections allowed CA2 injections.

Results demonstrate that the CA2 region of the mouse has connections similar to those reported from rat and monkey in which the dorsal CA2 pyramidal neurons project bilaterally

to regions CA3, CA2, and CA1 whereas CA2 receives bilateral hippocampal fibers from CA3 and CA2 (Ishizuka et al., 1990; Kondo et al., 2009; Li et al., 1994; Rosene and Van Hoesen, 1977). In agreement with previous studies, there is no projection from region CA1 to CA2.

The AAV-GFP tracing was especially useful in viewing the extent and relative distribution of efferent projections within the hippocampus. Our studies show that the CA2 projections to CA1, CA2 and CA3 are prominent and not as scattered projections as described previously in the rat (Ishizuka et al., 1990). We do not know whether this represents a species difference, difference in sensitivity of the methods, or a combination of both. The denser projection to the stratum oriens than stratum radiatum of CA1 from CA2 that we observed is consistent with a recent report that examined fiber projects from CA2 neurons using GFP expressed from the CACNG5 promoter (Shinohara et al., 2012). Moreover, unlike the CA3 to CA1 projection which shows a strong topographic pattern along septotemporal axis (Amaral and Witter, 1989), the CA2 to CA1 projections appear to have a more even distribution pattern. Early optical recording experiments found delayed signal propagation from CA3 to CA1 via CA2 (Sekino et al., 1997). Recent work has shown that the Schaffer collateral inputs from CA3 provide feed-forward inhibition to CA2 (Chevaleyre and Siegelbaum, 2010). These examples and the very intense interconnections of CA2 neurons with CA2 and CA3 and the one-way connection with CA1 support the need for continued investigations into this integral role of CA2 in memory.

In the classic model of hippocampal formation connectivity, the entorhinal cortex projects to the dentate gyrus for processing through the tri-synaptic excitatory pathway. Direct input from the entorhinal cortex to CA2 with subsequent excitation of CA1 pyramidal neurons has been reported in guinea pigs (Bartesaghi and Gessi, 2004; Bartesaghi et al., 2006) and mice (Chevaleyre and Siegelbaum, 2010), indicating that the classic model does not sufficiently cover all hippocampal afferents. It has been demonstrated that entorhinal cortical layer II spiny neurons project to the combined CA2/CA3 area (Steward and Scoville, 1976; Tamamaki and Nojyo, 1993). We refine these findings by showing that this input originates from both MEC and LEC layer II neurons without reciprocal efferents. The MEC and LEC behave as functionally distinct brain regions. For example, neurons in the MEC have fields that are spatially highly specific, while those in the LEC show weak spatial specificity (Fyhn et al., 2007; Hafting et al., 2005; Hargreaves et al., 2005) and respond preferentially to non-spatial variables, such as familiarity or odor identity (Young et al., 1997; Zhu et al., 1995). Their functional difference is a reflection of their differing inputs: MEC receives input from postrhinal cortex, which primarily transmits afferents from visual and parietal cortex (Kerr et al., 2007), whereas LEC receives direct olfactory input (Haberly and Price, 1977; Stranahan and Mattson, 2010) and encodes socially relevant odor information (Petrulis et al., 2005).

The Avpr1b is primarily expressed in the mouse CNS by CA2 pyramidal neurons (Young et al., 2006). Given that Avp facilitates long-term potentiation there (Zhao et al., 2010), and that its knockout impairs odor-related memory for temporal order as well as various social behaviors (DeVito et al., 2009; Wersinger et al., 2007; Wersinger et al., 2002; Wersinger et al., 2004; Wersinger et al., 2008), it is tempting to speculate that the convergence of both spatial and olfactory information from the entorhinal cortex in CA2 may enable formation and/or recall of social memories. The CA2 may, either by itself or in conjunction with CA1, create representations analogous to place cells that instead map social space to allow, for example, mapping of socially appropriate behaviors to their correct social context (e.g., recognition, affiliation and aggression).

The presence of Avpr1b in mouse dorsal CA2 gives rise to a question: from where does the Avp innervation arise? Avp fibers originating from the bed nucleus of the stria terminalis or medial amygdala have been reported to project to the ventral hippocampus but not the dorsal hippocampus (De Vries et al., 1985; Rood and De Vries, 2011). It was proposed that Avp could diffuse from the ventral to the dorsal hippocampus (Albeck et al., 1993). Our results now answer this question – vasopressinergic afferents to CA2 at least originate in the PVN. Targeting other sites of Avp expression with AAV-GFP or -cre-activated tdTomato may reveal additional sources of innervation. Two complementary approaches support this conclusion as discussed above. First, fluorogold is retrogradely transported to neurons within the PVN. Second, activation of the virally delivered, tdTomato anterograde tracer by cre recombinase only in Avp neurons leads to labeled fibers within CA2. In addition, Avpr1b expression is found in the immediately adjacent CA3 (Young et al., 2006), as are some fibers from the PVN in the current study. We will be interested to learn whether this vasopressinergic projection provides a constant or a variable facilitation of LTP at CA2 and, presumably, of social behaviors. In any case, the PVN is a site of convergence of information about an animal's internal and external milieus (Jankord and Herman, 2008; Ueta et al., 2011) and thus is well-situated to influence an animal's ability to form or recall a memory that would influence his subsequent behavior (e.g., recognize an intruder as a stranger and then engage in territorial aggression if fit).

We confirmed earlier findings from tracer studies that SUM innervates the dorsal CA2 (Haglund et al., 1984; Kiss et al., 2000; Magloczky et al., 1994; Ochiishi et al., 1999; Vertes, 1992). If the CA2 facilitates integration of spatial and chemosensory information from the entorhinal cortex, perhaps the input from the supramammillary nucleus contributes emotional salience. Neurons in the SUM respond to novelty (Ito et al., 2009), conditioned fear (Beck and Fibiger, 1995), and other various stressful situations (Cullinan et al., 1996; Miyata et al., 1998). This is consistent with SUM input from, among many areas, the infralimbic cortex, amygdala, lateral septum, medial preoptic area, other various hypothalamic nuclei, and the dorsal raphe nucleus (De Olmos et al., 2004; Hayakawa et al., 1993; Simerly and Swanson, 1988; Swanson and Cowan, 1979) in the rat.

Our study not only confirmed the CA2 afferent projection from the SUM, but also revealed a previously unknown efferent projection to SUM. This reciprocal connection, of course, could permit rapid feedback about various inputs to the CA2 and may be functionally distinct from the more indirect pathway from the SUM to dentate gyrus (Wyss et al., 1979) to CA3 to CA2 and back to SUM. This could convey specific social or emotional information (see above) or less specific but necessary information for hippocampal processing. The SUM strongly influences the hippocampal theta rhythm (Kirk and McNaughton, 1991; Kocsis and Vertes, 1994; Pan and McNaughton, 2002; Saji et al., 2000) which is important for forming memories (McNaughton et al., 2006) and generating behavior (Pan and McNaughton, 2002). Interestingly, vasopressin facilitates theta rhythm (Kosinski, 1986; Urban and De Wied, 1978; Urban, 1998) and may work through the Avpr1b expressed by CA2 pyramidal neurons (Young et al., 2006).

Previous studies showed that fibers originating from the median raphe are present in the CA2 in rats (Vertes et al., 1999) and hamsters (Morin and Meyer-Bernstein, 1999). Our study confirmed MRa terminals in CA2 using two retrograde tracers, one of which (green Retrobeads) is not known to be taken up by fibers of passage. We are not aware of similar retrograde analysis in other species. The MRa is known to inhibit hippocampal theta rhythm (Kinney et al., 1994; Maru et al., 1979). Furthermore, blockade of MRa activity also activates theta bursts in the medial septal nucleus (Kitchigina et al., 1999). Although we did not observe reciprocal connections between CA2 and the MRa (as between the CA2 and SUM and between CA2 and MS discussed just above and below, respectively), the CA2

could influence the MRa via the MS or SUM that do project to the MRa in rats (Behzadi et al., 1990; Marcinkiewicz et al., 1989). In addition, there is a projection to the MS from MRa in rats (Kohler et al., 1982; Segal and Landis, 1974) and hamsters (Morin and Meyer-Bernstein, 1999) enabling reciprocal innervations between these two nuclei.

The septal nuclei and both the vertical and horizontal limbs of the diagonal band of Broca have reciprocal innervations with the dorsal CA2. Specifically, the MS, VDB, and HDB project to the CA2 and the CA2 projects to the MS, LSD, VBD, and HDB. These results are consistent with previous studies ((Meibach and Siegel, 1977; Nyakas et al., 1987; Yoshida and Oka, 1995) and references therein). Furthermore, these areas provide cholinergic innervation to the hippocampus, affecting plasticity there (Drever et al., 2011). In particular, the nicotinic receptor subunits Chrna4 and Chrnb2 are prominently expressed in CA2 and the muscarinic receptor is highly expressed in CA2 (Lein et al., 2007). These cholinergic inputs to the hippocampus enhance attention and filtering of irrelevant information (Sarter et al., 2005). Projections from CA2 (and CA3) through the LSD to the ventral tegmental area may provide context for reward-seeking behavior (Luo et al., 2011). These are just a few of the many connections and functions associated with the septal nuclei and diagonal band of Broca (reviewed in (Medina and Abellan, 2012)) which likely influence hippocampal function at the dorsal CA2 in myriad ways.

Conclusions

The dorsal CA2 region likely serves a unique function within the hippocampus. It has its own set of connections, structures, and gene expression patterns that suggest a role in regulating social memories and behaviors. Our detailed analysis of the CA2 connections should provide a basis for more focused examinations of various observations or hypotheses with regard to CA2 functions, especially in genetically engineered mice. Our new findings of projections to and from the SUM and PVN, respectively, we hope will encourage further exploration of these pathways as well.

Acknowledgments

The NIMH Intramural Research Program supported this research (Z01-MH-002498-23 to WSY and Z01-MH-002947-23 to CRG).

The authors appreciate the helpful discussions with Drs. Zhang and Hernandez (National Autonomous Univ. of Mexico, Mexico City) about the use of fluorogold. We appreciate the expert technical help provided by June Song and invaluable discussions with and proof-readings by Drs. Éva Mezey, Miles Herkenham, Jerome Pagani and Sarah Williams.

Abbreviations used in this paper

AAV	adeno-associated virus
Avp	arginine vasopressin
Avpr1b	arginine vasopressin 1b receptor
CA2	hippocampal CA2 region
CA	Cornu Ammonis (also applies to CA1 and CA3)
CX	cortex
DG	dentate gyrus
df	dorsal fornix

dhc	dorsal hippocampal commissure
f	fornix
fi	fimbria
GFP	green fluorescent protein
HDB	horizontal limb of the nucleus of the diagonal band of Broca
LEC	lateral entorhinal cortex
LMol	Stratum lacunosum moleculare
LSD	lateral septal nucleus, dorsal part
MEC	medial entorhinal cortex
MM	mammillary body
MRa	median raphe nucleus
MS	medial septal nucleus
Or	stratum oriens
pm	principal mammillary tract
PVN	paraventricular nucleus of the hypothalamus
Py	stratum pyramidale
Rad	stratum radiatum
S	subiculum
Slu	stratum lucidum
SON	supraoptic nucleus
SUM	supramammillary nucleus
TS	triangular septal nucleus
VDB	vertical limb of the nucleus of the diagonal band of Broca
VPM	ventral posteromedial thalamic nucleus

Literature Cited

Albeck D, Bullock N, Marrs K, Cooper R, Smock T, De Vries GJ. Antidromic activation of a peptidergic pathway in the limbic system of the male rat. Brain Research. 1993; 606(1):171–174. [PubMed: 8461999]

Alisky JM, Hughes SM, Sauter SL, Jolly D, Dubensky TW Jr, Staber PD, Chiorini JA, Davidson BL. Transduction of murine cerebellar neurons with recombinant FIV and AAV5 vectors. Neuroreport. 2000; 11(12):2669–2673. [PubMed: 10976941]

Amaral DG, Witter MP. The three-dimensional organization of the hippocampal formation: a review of anatomical data. Neuroscience. 1989; 31(3):571–591. [PubMed: 2687721]

Andersen, P. The hippocampus book. Oxford; New York: Oxford University Press; 2007. p. 37-110.

Bartesaghi R, Gessi T. Parallel activation of field CA2 and dentate gyrus by synaptically elicited perforant path volleys. Hippocampus. 2004; 14(8):948–963. [PubMed: 15390176]

Bartesaghi R, Migliore M, Gessi T. Input-output relations in the entorhinal cortex-dentate-hippocampal system: evidence for a non-linear transfer of signals. Neuroscience. 2006; 142(1):247–265. [PubMed: 16844310]

Beck CH, Fibiger HC. Conditioned fear-induced changes in behavior and in the expression of the immediate early gene c-fos: with and without diazepam pretreatment. The Journal of neuroscience: the official journal of the Society for Neuroscience. 1995; 15(1 Pt 2):709–720. [PubMed: 7823174]

Behzadi G, Kalen P, Parvopassu F, Wiklund L. Afferents to the median raphe nucleus of the rat: retrograde cholera toxin and wheat germ conjugated horseradish peroxidase tracing, and selective D-[3H]aspartate labelling of possible excitatory amino acid inputs. Neuroscience. 1990; 37(1):77–100. [PubMed: 2243599]

Benes FM, Kwok EW, Vincent SL, Todtenkopf MS. A reduction of nonpyramidal cells in sector CA2 of schizophrenics and manic depressives. Biol Psychiatry. 1998; 44(2):88–97. [PubMed: 9646890]

Brierley, JB.; Graham, DI. Hypoxia and vascular disorders of the central nervous system. In: Adams, JH.; Corsellis, JAN.; Duchen, LW., editors. Greenfield's Neuropathology. 4. New York: John Wiley & Sons; 1984. p. 137

Chamberlin NL, Du B, de Lacalle S, Saper CB. Recombinant adeno-associated virus vector: use for transgene expression and anterograde tract tracing in the CNS. Brain Research. 1998; 793(1–2): 169–175. [PubMed: 9630611]

Chevaleyre V, Siegelbaum SA. Strong CA2 pyramidal neuron synapses define a powerful disynaptic cortico-hippocampal loop. Neuron. 2010; 66(4):560–572. [PubMed: 20510860]

Cullinan WE, Helmreich DL, Watson SJ. Fos expression in forebrain afferents to the hypothalamic paraventricular nucleus following swim stress. The Journal of comparative neurology. 1996; 368(1):88–99. [PubMed: 8725295]

Dam AM. Epilepsy and neuron loss in the hippocampus. Epilepsia. 1980; 21(6):617–629. [PubMed: 6777154]

De Olmos, J.; Beltramino, CA.; Alheid, G. Amygdala and extendedamygdala of the rat: a cytoarchitectonical, fibroarchitechtonical, and chemoarchitectonical survery. In: Paxinos, G., editor. The Rat Nervous System. 3. New Yorl: Elsevier; 2004. p. 509-603.

De Vries GJ, Buijs RM, Van Leeuwen FW, Caffe AR, Swaab DF. The vasopressinergic innervation of the brain in normal and castrated rats. J Comp Neurol. 1985; 233(2):236–254. [PubMed: 3882778]

Deng C, Rogers LJ. Differential sensitivities of the two visual pathways of the chick to labelling by fluorescent retrograde tracers. Journal of neuroscience methods. 1999; 89(1):75–86. [PubMed: 10476686]

DeVito LM, Konigsberg R, Lykken C, Sauvage M, Young WS 3rd, Eichenbaum H. Vasopressin 1b receptor knock-out impairs memory for temporal order. J Neurosci. 2009; 29(9):2676–2683. [PubMed: 19261862]

Drever BD, Riedel G, Platt B. The cholinergic system and hippocampal plasticity. Behav Brain Res. 2011; 221(2):505–514. [PubMed: 21130117]

Evans SJ, Choudary PV, Neal CR, Li JZ, Vawter MP, Tomita H, Lopez JF, Thompson RC, Meng F, Stead JD, Walsh DM, Myers RM, Bunney WE, Watson SJ, Jones EG, Akil H. Dysregulation of the fibroblast growth factor system in major depression. Proceedings of the National Academy of Sciences of the United States of America. 2004; 101(43):15506–15511. [PubMed: 15483108]

Franklin, KBJ.; Paxinos, G. The Mouse Brain in Stereotaxic Coordinates. San Diego: Academic Press; 2007.

Fyhn M, Hafting T, Treves A, Moser MB, Moser EI. Hippocampal remapping and grid realignment in entorhinal cortex. Nature. 2007; 446(7132):190–194. [PubMed: 17322902]

Gaughran F, Payne J, Sedgwick PM, Cotter D, Berry M. Hippocampal FGF-2 and FGFR1 mRNA expression in major depression, schizophrenia and bipolar disorder. Brain research bulletin. 2006; 70(3):221–227. [PubMed: 16861106]

Gong S, Doughty M, Harbaugh CR, Cummins A, Hatten ME, Heintz N, Gerfen CR. Targeting Cre recombinase to specific neuron populations with bacterial artificial chromosome constructs. J Neurosci. 2007; 27(37):9817–9823. [PubMed: 17855595]

Haberly LB, Price JL. The axonal projection patterns of the mitral and tufted cells of the olfactory bulb in the rat. Brain Res. 1977; 129(1):152–157. [PubMed: 68803]

Hafting T, Fyhn M, Molden S, Moser MB, Moser EI. Microstructure of a spatial map in the entorhinal cortex. Nature. 2005; 436(7052):801–806. [PubMed: 15965463]

Haglund L, Swanson LW, Kohler C. The projection of the supramammillary nucleus to the hippocampal formation: an immunohistochemical and anterograde transport study with the lectin PHA-L in the rat. J Comp Neurol. 1984; 229(2):171–185. [PubMed: 6501599]

Hargreaves EL, Rao G, Lee I, Knierim JJ. Major dissociation between medial and lateral entorhinal input to dorsal hippocampus. Science. 2005; 308(5729):1792–1794. [PubMed: 15961670]

Hayakawa T, Ito H, Zyo K. Neuroanatomical study of afferent projections to the supramammillary nucleus of the rat. Anat Embryol (Berl). 1993; 188(2):139–148. [PubMed: 8214629]

Honkaniemi J, Sharp FR. Prolonged expression of zinc finger immediate-early gene mRNAs and decreased protein synthesis following kainic acid induced seizures. Eur J Neurosci. 1999; 11(1): 10–17. [PubMed: 9987007]

Ishizuka N, Weber J, Amaral DG. Organization of intrahippocampal projections originating from CA3 pyramidal cells in the rat. J Comp Neurol. 1990; 295(4):580–623. [PubMed: 2358523]

Ito M, Shirao T, Doya K, Sekino Y. Three-dimensional distribution of Fos-positive neurons in the supramammillary nucleus of the rat exposed to novel environment. Neuroscience research. 2009; 64(4):397–402. [PubMed: 19409426]

Jankord R, Herman JP. Limbic regulation of hypothalamo-pituitary-adrenocortical function during acute and chronic stress. Annals of the New York Academy of Sciences. 2008; 1148:64–73. [PubMed: 19120092]

Kaspar BK, Erickson D, Schaffer D, Hinh L, Gage FH, Peterson DA. Targeted retrograde gene delivery for neuronal protection. Mol Ther. 2002; 5(1):50–56. [PubMed: 11786045]

Kerr KM, Agster KL, Furtak SC, Burwell RD. Functional neuroanatomy of the parahippocampal region: the lateral and medial entorhinal areas. Hippocampus. 2007; 17(9):697–708. [PubMed: 17607757]

Kinney GG, Kocsis B, Vertes RP. Injections of excitatory amino acid antagonists into the median raphe nucleus produce hippocampal theta rhythm in the urethane-anesthetized rat. Brain Research. 1994; 654(1):96–104. [PubMed: 7982102]

Kirk IJ, McNaughton N. Supramammillary cell firing and hippocampal rhythmical slow activity. Neuroreport. 1991; 2(11):723–725. [PubMed: 1810464]

Kiss J, Csaki A, Bokor H, Shanabrough M, Leranth C. The supramammillo-hippocampal and supramammillo-septal glutamatergic/aspartatergic projections in the rat: a combined [3H]D-aspartate autoradiographic and immunohistochemical study. Neuroscience. 2000; 97(4):657–669. [PubMed: 10842010]

Kitchigina VF, Kudina TA, Kutyreva EV, Vinogradova OS. Neuronal activity of the septal pacemaker of theta rhythm under the influence of stimulation and blockade of the median raphe nucleus in the awake rabbit. Neuroscience. 1999; 94(2):453–463. [PubMed: 10579208]

Klein RL, Meyer EM, Peel AL, Zolotukhin S, Meyers C, Muzyczka N, King MA. Neuron-specific transduction in the rat septohippocampal or nigrostriatal pathway by recombinant adeno-associated virus vectors. Experimental neurology. 1998; 150(2):183–194. [PubMed: 9527887]

Kocsis B, Vertes RP. Characterization of neurons of the supramammillary nucleus and mammillary body that discharge rhythmically with the hippocampal theta rhythm in the rat. J Neurosci. 1994; 14(11 Pt 2):7040–7052. [PubMed: 7965097]

Kohler C, Chan-Palay V, Steinbusch H. The distribution and origin of serotonin-containing fibers in the septal area: a combined immunohistochemical and fluorescent retrograde tracing study in the rat. The Journal of comparative neurology. 1982; 209(1):91–111. [PubMed: 6749914]

Kondo H, Lavenex P, Amaral DG. Intrinsic connections of the macaque monkey hippocampal formation: II. CA3 connections. J Comp Neurol. 2009; 515(3):349–377. [PubMed: 19425110]

Kosinski S. Effects of intracerebroventricular administration of vasopressin and oxytocin on the extinction of hippocampal theta rhythm in rabbits. Acta Neurobiol Exp (Wars). 1986; 46(1):27–35. [PubMed: 3739759]

Leak RK, Moore RY. Identification of retinal ganglion cells projecting to the lateral hypothalamic area of the rat. Brain Research. 1997; 770(1–2):105–114. [PubMed: 9372209]

Lein E, Callaway E, Albright T, Gage F. Redefining the boundaries of the hippocampal CA2 subfield in the mouse using gene expression and 3-dimensional reconstruction. J Comp Neurol. 2005a; 485(1):1–10. [PubMed: 15776443]

Lein E, Zhao X, Gage F. Defining a molecular atlas of the hippocampus using DNA microarrays and high-throughput in situ hybridization. J Neurosci. 2004; 24(15):3879–3889. [PubMed: 15084669]

Lein ES, Callaway EM, Albright TD, Gage FH. Redefining the boundaries of the hippocampal CA2 subfield in the mouse using gene expression and 3-dimensional reconstruction. J Comp Neurol. 2005b; 485(1):1–10. [PubMed: 15776443]

Lein ES, Hawrylycz MJ, Ao N, Ayres M, Bensinger A, Bernard A, Boe AF, Boguski MS, Brockway KS, Byrnes EJ, Chen L, Chen TM, Chin MC, Chong J, Crook BE, Czaplinska A, Dang CN, Datta S, Dee NR, Desaki AL, Desta T, Diep E, Dolbeare TA, Donelan MJ, Dong HW, Dougherty JG, Duncan BJ, Ebbert AJ, Eichele G, Estin LK, Faber C, Facer BA, Fields R, Fischer SR, Fliss TP, Frensley C, Gates SN, Glattfelder KJ, Halverson KR, Hart MR, Hohmann JG, Howell MP, Jeung DP, Johnson RA, Karr PT, Kawal R, Kidney JM, Knapik RH, Kuan CL, Lake JH, Laramee AR, Larsen KD, Lau C, Lemon TA, Liang AJ, Liu Y, Luong LT, Michaels J, Morgan JJ, Morgan RJ, Mortrud MT, Mosqueda NF, Ng LL, Ng R, Orta GJ, Overly CC, Pak TH, Parry SE, Pathak SD, Pearson OC, Puchalski RB, Riley ZL, Rockett HR, Rowland SA, Royall JJ, Ruiz MJ, Sarno NR, Schaffnit K, Shapovalova NV, Sivisay T, Slaughterbeck CR, Smith SC, Smith KA, Smith BI, Sodt AJ, Stewart NN, Stumpf KR, Sunkin SM, Sutram M, Tam A, Teemer CD, Thaller C, Thompson CL, Varnam LR, Visel A, Whitlock RM, Wohnoutka PE, Wolkey CK, Wong VY, Wood M, Yaylaoglu MB, Young RC, Youngstrom BL, Yuan XF, Zhang B, Zwingman TA, Jones AR. Genome-wide atlas of gene expression in the adult mouse brain. Nature. 2007; 445(7124):168–176. [PubMed: 17151600]

Li XG, Somogyi P, Ylinen A, Buzsaki G. The hippocampal CA3 network: an in vivo intracellular labeling study. The Journal of comparative neurology. 1994; 339(2):181–208. [PubMed: 8300905]

Liou YJ, Chen TJ, Tsai SJ, Yu YW, Cheng CY, Hong CJ. Support for the involvement of the KCNK2 gene in major depressive disorder and response to antidepressant treatment. Pharmacogenet Genomics. 2009; 19(10):735–741. [PubMed: 19741570]

Lorente, dN. Studies on the structure of the cerebral cortex. II. Continuation of the study of the ammonic system. journal of Psychological Neurology. 1934; 46:113–177.

Luo AH, Tahsili-Fahadan P, Wise RA, Lupica CR, Aston-Jones G. Linking context with reward: a functional circuit from hippocampal CA3 to ventral tegmental area. Science. 2011; 333(6040): 353–357. [PubMed: 21764750]

Magloczky Z, Acsady L, Freund TF. Principal cells are the postsynaptic targets of supramammillary afferents in the hippocampus of the rat. Hippocampus. 1994; 4(3):322–334. [PubMed: 7531093]

Marcinkiewicz M, Morcos R, Chretien M. CNS connections with the median raphe nucleus: retrograde tracing with WGA-apoHRP-Gold complex in the rat. The Journal of comparative neurology. 1989; 289(1):11–35. [PubMed: 2478595]

Maru E, Takahashi LK, Iwahara S. Effects of median raphe nucleus lesions on hippocampal EEG in the freely moving rat. Brain Research. 1979; 163(2):223–234. [PubMed: 218681]

McNaughton N, Ruan M, Woodnorth MA. Restoring theta-like rhythmicity in rats restores initial learning in the Morris water maze. Hippocampus. 2006; 16(12):1102–1110. [PubMed: 17068783]

Medina, L.; Abellan, A. Subpallial structures. In: Watson, C.; Paxinos, G.; Puelles, L., editors. THe Mouse Nervous System. NewYork: Academic Prss; 2012. p. 173-220.

Meibach RC, Siegel A. Efferent connections of the septal area in the rat: an analysis utilizing retrograde and anterograde transport methods. Brain Res. 1977; 119(1):1–20. [PubMed: 63306]

Meldrum, BS.; Corsellis, JAN. Epilepsy. In: Adams, JH.; Corsellis, JAN.; Duchen, LW., editors. Greenfield's Neuropathology. 4. New York: John Wiley & Sons; 1984. p. 928-929.

Miyata S, Ishiyama M, Shibata M, Nakashima T, Kiyohara T. Infant cold exposure changes Fos expression to acute cold stimulation in adult hypothalamic brain regions. Neuroscience research. 1998; 31(3):219–225. [PubMed: 9809667]

Morin LP, Meyer-Bernstein EL. The ascending serotonergic system in the hamster: comparison with projections of the dorsal and median raphe nuclei. Neuroscience. 1999; 91(1):81–105. [PubMed: 10336062]

Nyakas C, Luiten PG, Spencer DG, Traber J. Detailed projection patterns of septal and diagonal band efferents to the hippocampus in the rat with emphasis on innervation of CA1 and dentate gyrus. Brain research bulletin. 1987; 18(4):533–545. [PubMed: 3607523]

Ochiishi T, Saitoh Y, Yukawa A, Saji M, Ren Y, Shirao T, Miyamoto H, Nakata H, Sekino Y. High level of adenosine A1 receptor-like immunoreactivity in the CA2/CA3a region of the adult rat hippocampus. Neuroscience. 1999; 93(3):955–967. [PubMed: 10473260]

Pan WX, McNaughton N. The role of the medial supramammillary nucleus in the control of hippocampal theta activity and behaviour in rats. Eur J Neurosci. 2002; 16(9):1797–1809. [PubMed: 12431233]

Perlis RH, Moorjani P, Fagerness J, Purcell S, Trivedi MH, Fava M, Rush AJ, Smoller JW. Pharmacogenetic analysis of genes implicated in rodent models of antidepressant response: association of TREK1 and treatment resistance in the STAR(*)D study. Neuropsychopharmacology: official publication of the American College of Neuropsychopharmacology. 2008; 33(12):2810–2819. [PubMed: 18288090]

Petrulis A, Alvarez P, Eichenbaum H. Neural correlates of social odor recognition and the representation of individual distinctive social odors within entorhinal cortex and ventral subiculum. Neuroscience. 2005; 130(1):259–274. [PubMed: 15561442]

Rood BD, De Vries GJ. Vasopressin innervation of the mouse (Mus musculus) brain and spinal cord. J Comp Neurol. 2011; 519(12):2434–2474. [PubMed: 21456024]

Rosene DL, Van Hoesen GW. Hippocampal efferents reach widespread areas of cerebral cortex and amygdala in the rhesus monkey. Science. 1977; 198(4314):315–317. [PubMed: 410102]

Saji M, Kobayashi S, Ohno K, Sekino Y. Interruption of supramammillohippocampal afferents prevents the genesis and spread of limbic seizures in the hippocampus via a disinhibition mechanism. Neuroscience. 2000; 97(3):437–445. [PubMed: 10828527]

Sarter M, Hasselmo ME, Bruno JP, Givens B. Unraveling the attentional functions of cortical cholinergic inputs: interactions between signal-driven and cognitive modulation of signal detection. Brain Res Brain Res Rev. 2005; 48(1):98–111. [PubMed: 15708630]

Segal M, Landis SC. Afferents to the septal area of the rat studied with the method of retrograde axonal transport of horseradish peroxidase. Brain Research. 1974; 82(2):263–268. [PubMed: 4140749]

Sekino Y, Obata K, Tanifuji M, Mizuno M, Murayama J. Delayed signal propagation via CA2 in rat hippocampal slices revealed by optical recording. J Neurophysiol. 1997; 78(3):1662–1668. [PubMed: 9310451]

Shinohara Y, Hosoya A, Yahagi K, Ferecsko AS, Yaguchi K, Sik A, Itakura M, Takahashi M, Hirase H. Hippocampal CA3 and CA2 have distinct bilateral innervation patterns to CA1 in rodents. The European journal of neuroscience. 2012; 35(5):702–710. [PubMed: 22339771]

Simerly RB, Swanson LW. Projections of the medial preoptic nucleus: a Phaseolus vulgaris leucoagglutinin anterograde tract-tracing study in the rat. The Journal of comparative neurology. 1988; 270(2):209–242. [PubMed: 3259955]

Simons SB, Caruana DA, Zhao M, Dudek SM. Caffeine-induced synaptic potentiation in hippocampal CA2 neurons. Nat Neurosci. 2012; 15(1):23–25. [PubMed: 22101644]

Sperk G. Kainic acid seizures in the rat. Prog Neurobiol. 1994; 42(1):1–32. [PubMed: 7480784]

Steward O, Scoville SA. Cells of origin of entorhinal cortical afferents to the hippocampus and fascia dentata of the rat. J Comp Neurol. 1976; 169(3):347–370. [PubMed: 972204]

Stranahan AM, Mattson MP. Selective vulnerability of neurons in layer II of the entorhinal cortex during aging and Alzheimer's disease. Neural Plast. 2010; 2010:108190. [PubMed: 21331296]

Swanson LW, Cowan WM. The connections of the septal region in the rat. The Journal of comparative neurology. 1979; 186(4):621–655. [PubMed: 15116692]

Talley EM, Solorzano G, Lei Q, Kim D, Bayliss DA. CNS distribution of members of the two-pore-domain (KCNK) potassium channel family. J Neurosci. 2001; 21(19):7491–7505. [PubMed: 11567039]

Tamamaki N, Nojyo Y. Projection of the entorhinal layer II neurons in the rat as revealed by intracellular pressure-injection of neurobiotin. Hippocampus. 1993; 3(4):471–480. [PubMed: 8269038]

Thompson CL, Pathak SD, Jeromin A, Ng LL, MacPherson CR, Mortrud MT, Cusick A, Riley ZL, Sunkin SM, Bernard A, Puchalski RB, Gage FH, Jones AR, Bajic VB, Hawrylycz MJ, Lein ES. Genomic anatomy of the hippocampus. Neuron. 2008; 60(6):1010–1021. [PubMed: 19109908]

Turner CA, Clinton SM, Thompson RC, Watson SJ Jr, Akil H. Fibroblast growth factor-2 (FGF2) augmentation early in life alters hippocampal development and rescues the anxiety phenotype in vulnerable animals. Proceedings of the National Academy of Sciences of the United States of America. 2011; 108(19):8021–8025. [PubMed: 21518861]

Ueta Y, Dayanithi G, Fujihara H. Hypothalamic vasopressin response to stress and various physiological stimuli: visualization in transgenic animal models. Hormones and Behavior. 2011; 59(2):221–226. [PubMed: 21185297]

Urban I, De Wied D. Neuropeptides: effects on paradoxical sleep and theta rhythm in rats. Pharmacol Biochem Behav. 1978; 8(1):51–59. [PubMed: 203949]

Urban IJ. Effects of vasopressin and related peptides on neurons of the rat lateral septum and ventral hippocampus. Prog Brain Res. 1998; 119:285–310. [PubMed: 10074795]

van Strien NM, Cappaert NL, Witter MP. The anatomy of memory: an interactive overview of the parahippocampal-hippocampal network. Nat Rev Neurosci. 2009; 10(4):272–282. [PubMed: 19300446]

Vertes RP. PHA-L analysis of projections from the supramammillary nucleus in the rat. The Journal of comparative neurology. 1992; 326(4):595–622. [PubMed: 1484125]

Vertes RP, Fortin WJ, Crane AM. Projections of the median raphe nucleus in the rat. The Journal of comparative neurology. 1999; 407(4):555–582. [PubMed: 10235645]

Wersinger SR, Caldwell HK, Christiansen M, Young WS 3rd. Disruption of the vasopressin 1b receptor gene impairs the attack component of aggressive behavior in mice. Genes Brain Behav. 2007; 6(7):653–660. [PubMed: 17284170]

Wersinger SR, Ginns EI, O'Carroll AM, Lolait SJ, Young WS 3rd. Vasopressin V1b receptor knockout reduces aggressive behavior in male mice. Mol Psychiatry. 2002; 7(9):975–984. [PubMed: 12399951]

Wersinger SR, Kelliher KR, Zufall F, Lolait SJ, O'Carroll AM, Young WS 3rd. Social motivation is reduced in vasopressin 1b receptor null mice despite normal performance in an olfactory discrimination task. Horm Behav. 2004; 46(5):638–645. [PubMed: 15555506]

Wersinger SR, Temple JL, Caldwell HK, Young WS 3rd. Inactivation of the oxytocin and the vasopressin (Avp) 1b receptor genes, but not the Avp 1a receptor gene, differentially impairs the Bruce effect in laboratory mice (Mus musculus). Endocrinology. 2008; 149(1):116–121. [PubMed: 17947352]

Williamson A, Spencer DD. Electrophysiological characterization of CA2 pyramidal cells from epileptic humans. Hippocampus. 1994; 4(2):226–237. [PubMed: 7951697]

Wyss JM, Swanson LW, Cowan WM. Evidence for an input to the molecular layer and the stratum granulosum of the dentate gyrus from the supramammillary region of the hypothalamus. Anat Embryol (Berl). 1979; 156(2):165–176. [PubMed: 464319]

Yoshida K, Oka H. Topographical projections from the medial septum-diagonal band complex to the hippocampus: a retrograde tracing study with multiple fluorescent dyes in rats. Neuroscience research. 1995; 21(3):199–209. [PubMed: 7753501]

Young BJ, Otto T, Fox GD, Eichenbaum H. Memory representation within the parahippocampal region. The Journal of neuroscience: the official journal of the Society for Neuroscience. 1997; 17(13):5183–5195. [PubMed: 9185556]

Young WS, Li J, Wersinger SR, Palkovits M. The vasopressin 1b receptor is prominent in the hippocampal area CA2 where it is unaffected by restraint stress or adrenalectomy. Neuroscience. 2006; 143(4):1031–1039. [PubMed: 17027167]

Zhang L, Hernandez VS. Vasopressinergic innervations to hippocampus: An anatomical study on its origin, distribution and synaptic targets. Soc Neurosci Abstracts. 2011

Zhao M, Choi YS, Obrietan K, Dudek SM. Synaptic plasticity (and the lack thereof) in hippocampal CA2 neurons. J Neurosci. 2007; 27(44):12025–12032. [PubMed: 17978044]

Zhao, M.; Young, WS.; Dudek, SM. Vasopressin Induces Synaptic Potentiation in Hippocampal CA2 Neurons. Soc Neurosci Annual Meeting; San Diego, CA. 2010.

Zhao X, Lein ES, He A, Smith SC, Aston C, Gage FH. Transcriptional profiling reveals strict boundaries between hippocampal subregions. J Comp Neurol. 2001; 441(3):187–196. [PubMed: 11745644]

Zhu XO, Brown MW, Aggleton JP. Neuronal signalling of information important to visual recognition memory in rat rhinal and neighbouring cortices. The European journal of neuroscience. 1995; 7(4):753–765. [PubMed: 7620624]

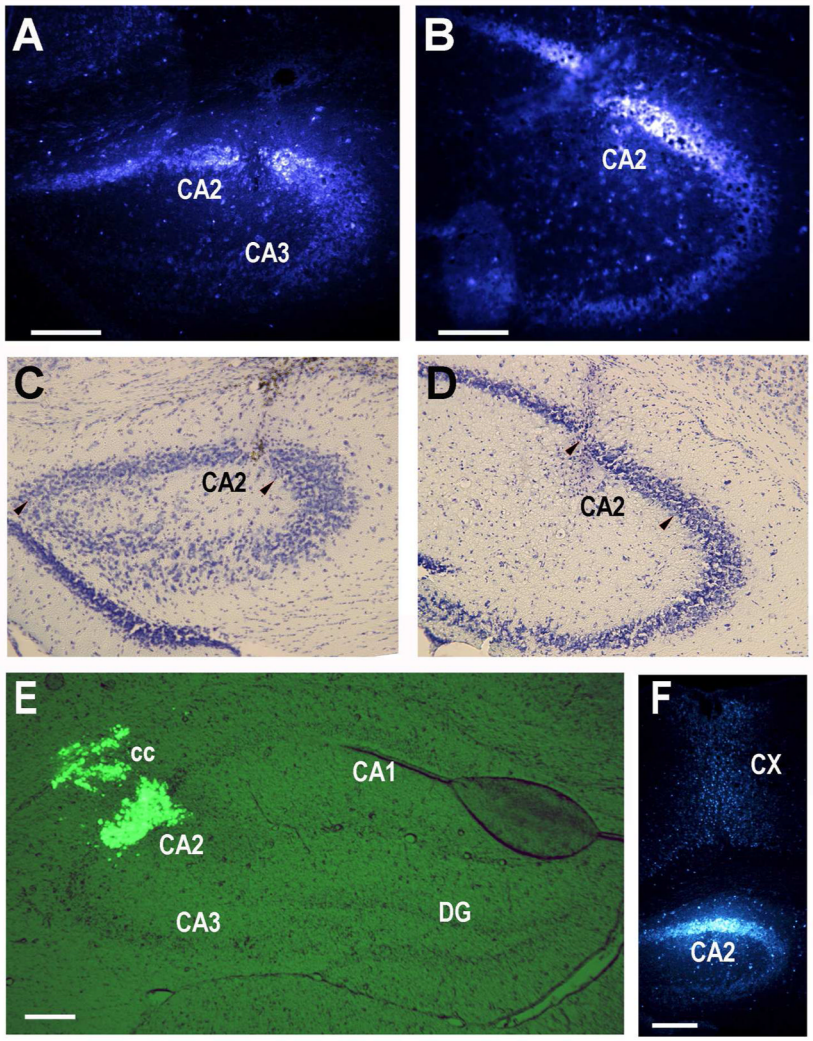

Fig. 1.

Retrograde tracer injections into the dorsal hippocampal CA2 region. A. 10nl of 4% fluorogold tracer injected into the dorsomedial CA2 at 0.80, −1.06, −1.76mm (site 1; see Methods for explanation of coordinates). B. 10nl of 4% fluorogold tracer injected into the dorsolateral CA2 at 1.85, −1.70, −1.85mm (site 2). C, D. Nissl staining of sections in panels A and B with CA2 delineated by pairs of arrowheads. E. 120nl of green Retrobeads injected into site 2. A slightly leak into the corpus callosum (cc) is visible, but CA2 is well targeted. F. 10nl of 4% fluorogold tracer injected into site 1 showing the slight leak in the cortex along the needle track. CX: cortex. Scale bars equal 100 μm (for each Nissl section, use the scale bar in the panel above).

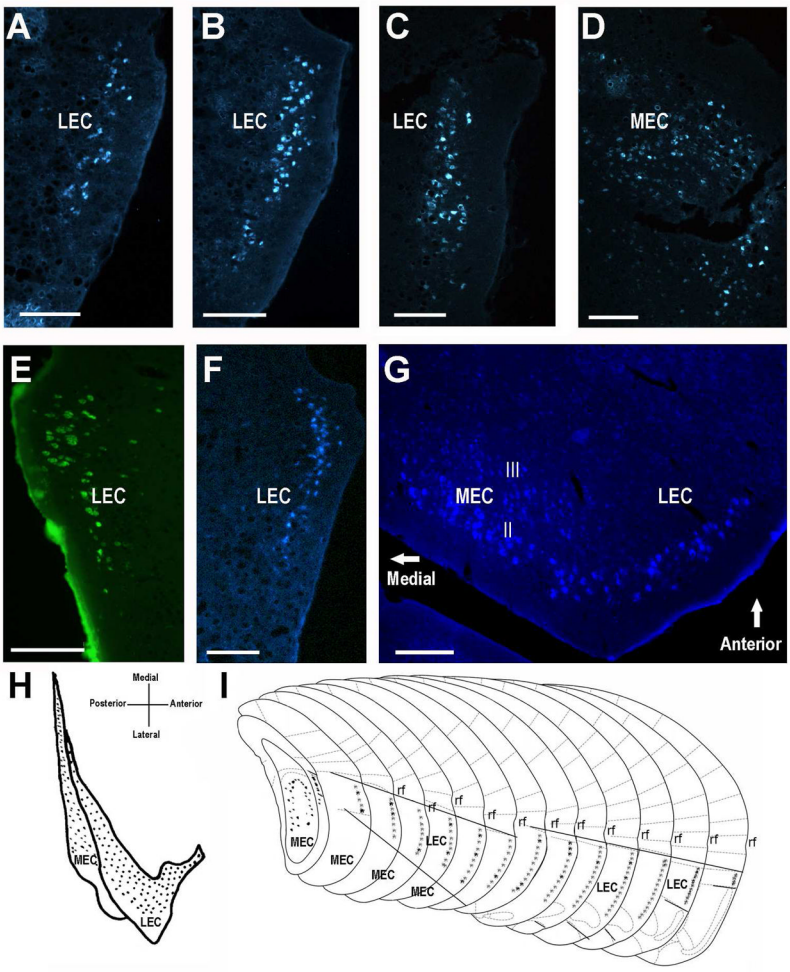

Fig. 2.

CA2 afferent projections from the medial and lateral entorhinal cortex layer II neurons. A–D. Coronal sections of entorhinal cortex retrogradely labeled with fluorogold from a site 2 CA2 injection (Fig. 1B). A to D is from anterior to posterior. E. LEC labeling using green Retrobeads injected into CA2 site 2 (Fig. 1E). F. Coronal section of fluorogold-labeled entorhinal cortex from site 1 CA2 injection (Fig. 1A). G. A horizontal section showing fluorogold-labeled layer II neurons of both MEC and LEC. Fewer, less faintly labeled cells are found in layer III. Scale bars equal 100 μm. H. On a flattened schematic map of entorhinal cortex, the dotted areas show the retrograde tracer-positive layer II neurons of MEC and LEC. I. Schematic presentation (modified from (Franklin and Paxinos, 2007) with permission) of the relative positions of the labeled layer II neurons in consecutive coronal sections. The regions between solid straight lines bound the lateral entorhinal cortex region. The ventral third of both MEC and LEC did not contain labeled neurons. rf=rhinal fissure.

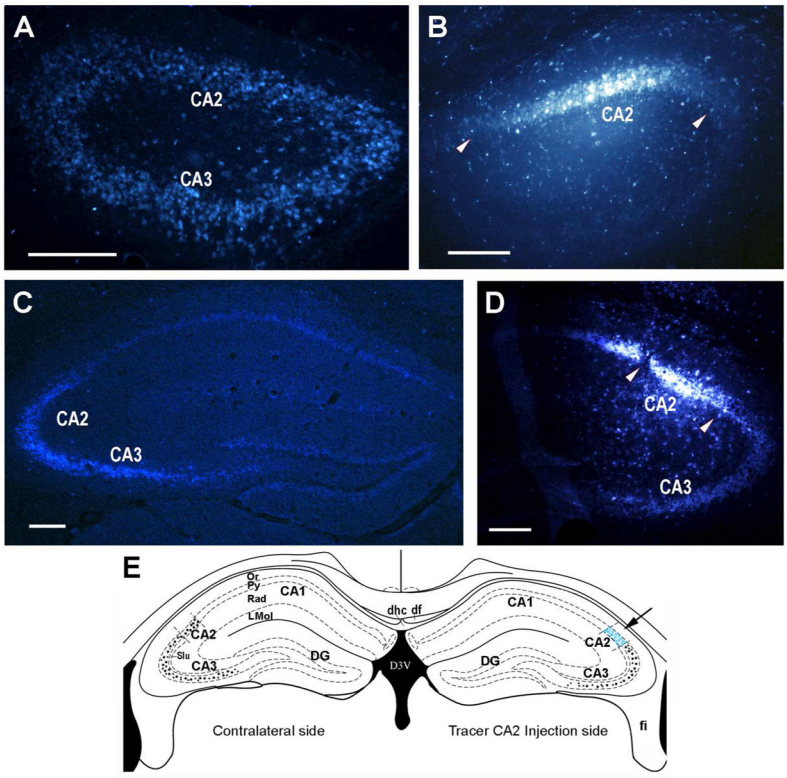

Fig. 3.

The intrahippocampal afferent connections revealed by fluorogold CA2 injections. A. Contralateral CA2 and CA3 were labeled by tracer injection at CA2 site 1 injection (panel B). B. The CA2 injection at site 1 (a pair of arrowheads delineate CA2). C. Contralateral CA2 and CA3 were labeled by tracer injection at CA2 site 2 (panel D). D. The CA2 injection at site 2 as delineated between the arrowheads (a slightly leak into the adjacent CA1 neurons is visible). No labeling of CA1 neurons was seen in either ipsilateral or contralateral sides. Panel D also shows labeled CA3 neurons after this CA2 injection. E. Schematic (modified from (Franklin and Paxinos, 2007) with permission) illustrating projections to the CA2 from the contralateral CA2 and CA3 and ipsilateral CA3 (Projecting cells represented as black dots. The shaded region (pointed to by arrow) of the drawing indicates a retrograde tracer injection site). Scale bars equal 100 μm.

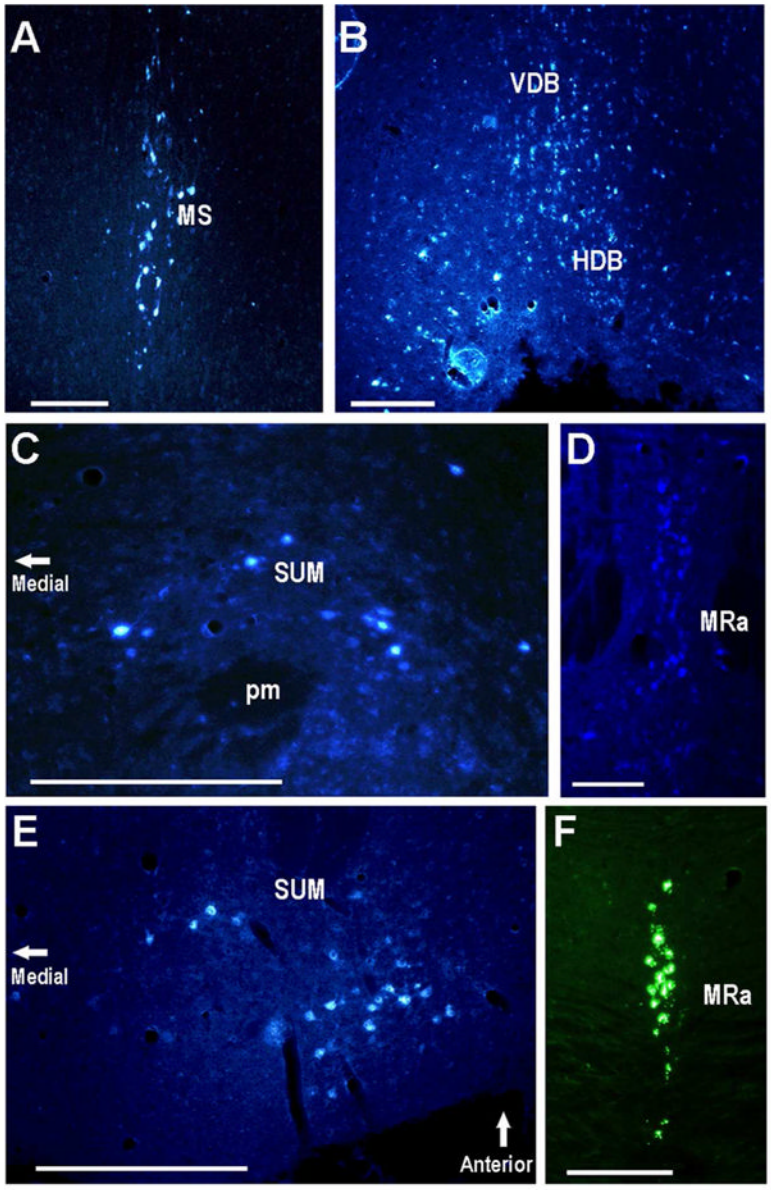

Fig. 4.

The medial septal nucleus, supramammillary nucleus, and median raphe project to the CA2. Areas with labeled neurons after CA2 injections (Fluorogold in all panels except green Retrobeads in panel F): A. Coronal section containing labeled neurons in the MS. B. Coronal section containing labeled neurons in the HDB and VDB. C. Coronal section showing large labeled neurons of the SUM. D,F. MRa labeled neurons in coronal sections. E. Horizontal section containing labeled neurons in the SUM. Scale bars equal 100 μm.

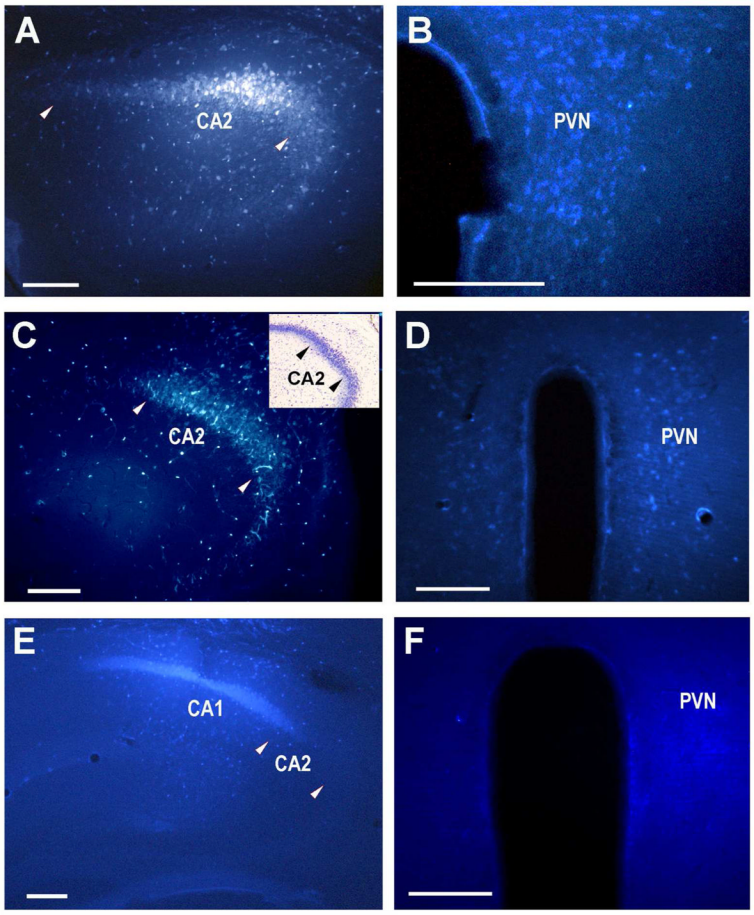

Fig. 5.

The paraventricular nucleus of the hypothalamus projects bilaterally to CA2. Single injections of 20nl of 1% fluorogold in 0.2M sodium cacodylate buffer were made 1 month prior to removal of brains. A. Injection into the dorsomedial CA2 (0.80, −1.06, −1.73mm (arrowheads delineate the CA2 region). B. Retrogradely labeled neurons in the PVN. C. Injection into the dorsolateral CA2 (1.85, −1.70, −1.85mm; the two arrowheads delineate the CA2 region and the small insert shows the CA2 region Nissl stained section). D. Retrogradely labeled neurons in the PVN with more labeling ipsilaterally than contralaterally. E. Injection of fluorogold tracer into CA1. F. No labeled cells were seen in the PVN after the CA1 tracer. After 4 weeks, the fluorogold was metabolized or had left the retrogradely labeled neurons of CA2 (panel E) or in CA3 (panels A and C), and is diminished at the sites of injection. Scale bars equal 100 μm.

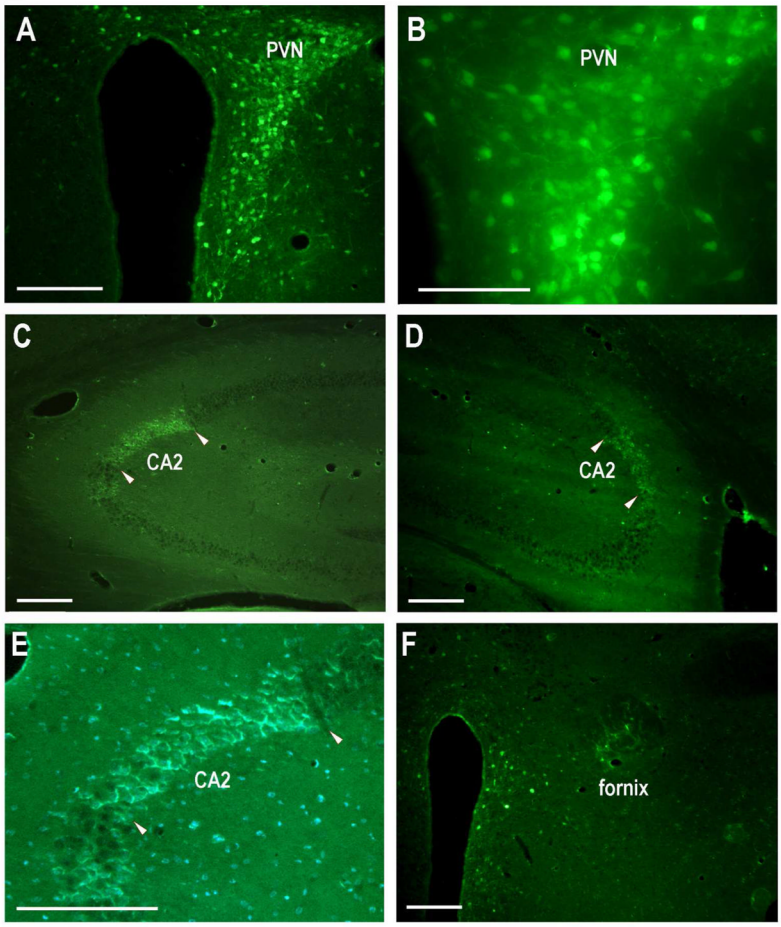

Fig. 6.

The paraventricular nucleus projects to the dorsal CA2 regions bilaterally. A. Unilateral AAV-GFP injection (200nl) into the PVN and surrounding region (higher magnification in B). C. GFP-positive fibers within the contralateral CA2 pyramidal layer. The CA2 regions are delineated by pairs of arrowheads. Note some fibers in the immediately adjacent CA3. D. GFP-positive fibers within the ipsilateral CA2 and immediately adjacent CA3 pyramidal layer. E. Pyramidal neurons stained with DAPI have surrounding GFP fibers. F. The fornix anterior to the PVN injection site contains GFP-positive fibers. However, the fornix posterior to the PVN injection site did not (not shown). Scale bars equal 100 μm in A, C, D, F; 50 μm in B, E.

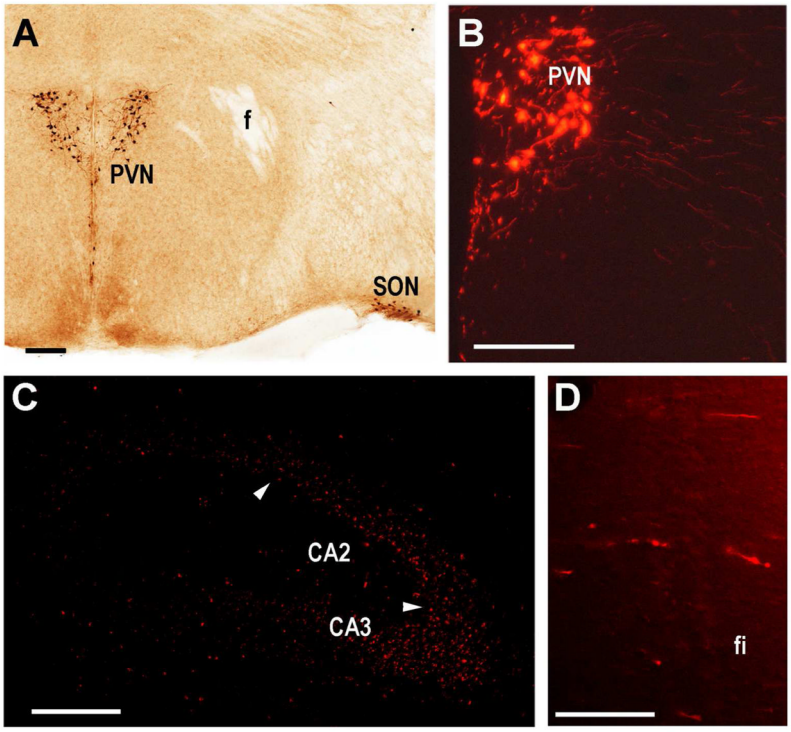

Fig. 7.

Vasopressinergic neuronal projections from PVN to CA2. A. Detection of Cre expression within the PVN driven by the Avp promoter in the GENSAT transgenic mouse line QZ27 as described (Gong et al., 2007). B. Cre activation of tdTomato delivered by AAV into the PVN of a QZ27 mouse showing large and smaller labeled neurons with fibers exiting. C. Labeled fibers within the ipsilateral dorsolateral CA2 (delineated by white arrowheads) and immediately adjacent CA3. D. Labeled fibers in the ipsilateral fimbria. Scale bars equal 100 μm except D (50μm).

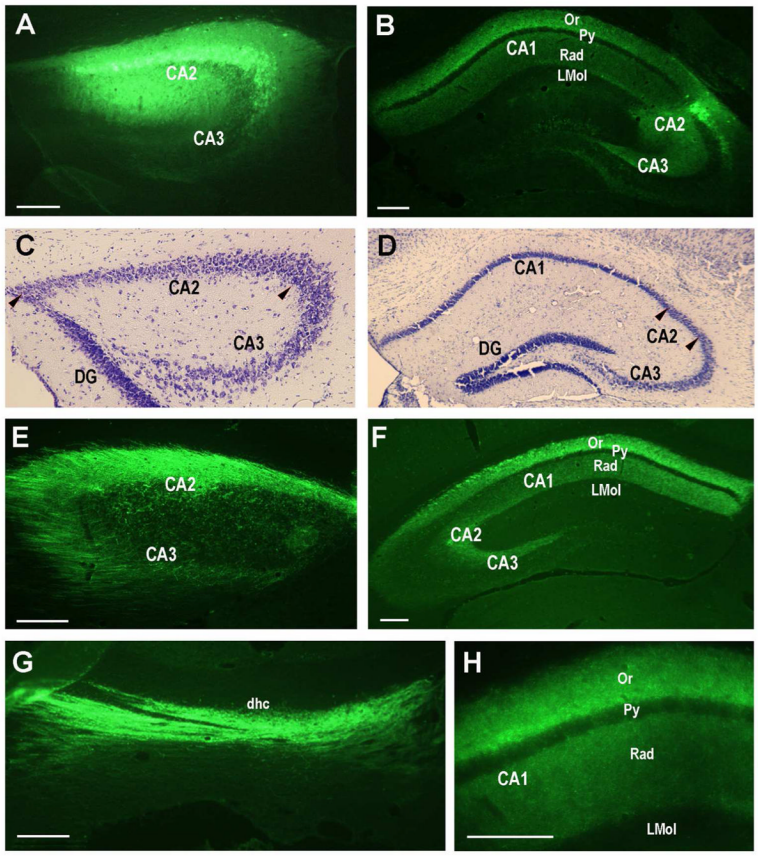

Fig. 8.

Unilateral pairs of AAV-GFP injections into the dorsal CA2 display extensive neuronal efferent projections within the hippocampus. A. AAV-GFP injection (400 nl) at dorsomedial CA2. B. The AAV-GFP injection (400 nl) at dorsolateral CA2 and fibers present in CA1, CA2 and CA3. C, D. Nissl stained sections of adjacent to the sections of panels A and B with the CA2 regions delineated by pairs arrowheads. E. Extensive projections to the contralateral dorsomedial CA2 and CA3. F. Extensive projections to the contralateral dorsolateral CA1, CA2 and CA3. G. Heavily labeled GFP-positive axons travel to the contralateral hippocampus through the hippocampal commissure. H. Higher magnification of the contralateral CA1 showing layer-specific CA2 innervation. The stratum oriens receives a heavier projection than the stratum radiatum, the stratum pyramidale receives very little CA2 input. Scale bars equal 100 μm (for each Nissl section, use the scale bar in the panel above).

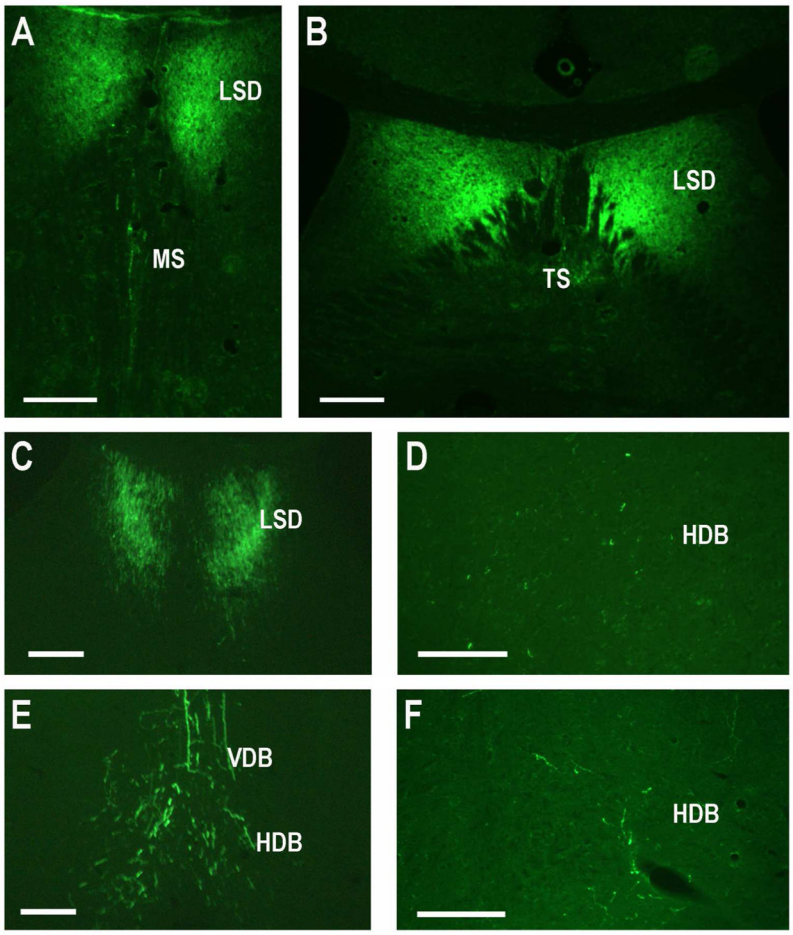

Fig. 9.

Unilateral AAV-GFP injections into the dorsal CA2 (the injections indicated in Fig. 8) display prominent efferent projections to septal areas. A – C. Bilateral efferent projections to the medial, lateral and triangular septal regions. D – F. Bilateral efferent projections to the horizontal and vertical limbs of the diagonal band of Broca (D, contralateral; F ipsilateral). Scale bars equal 100 μm.

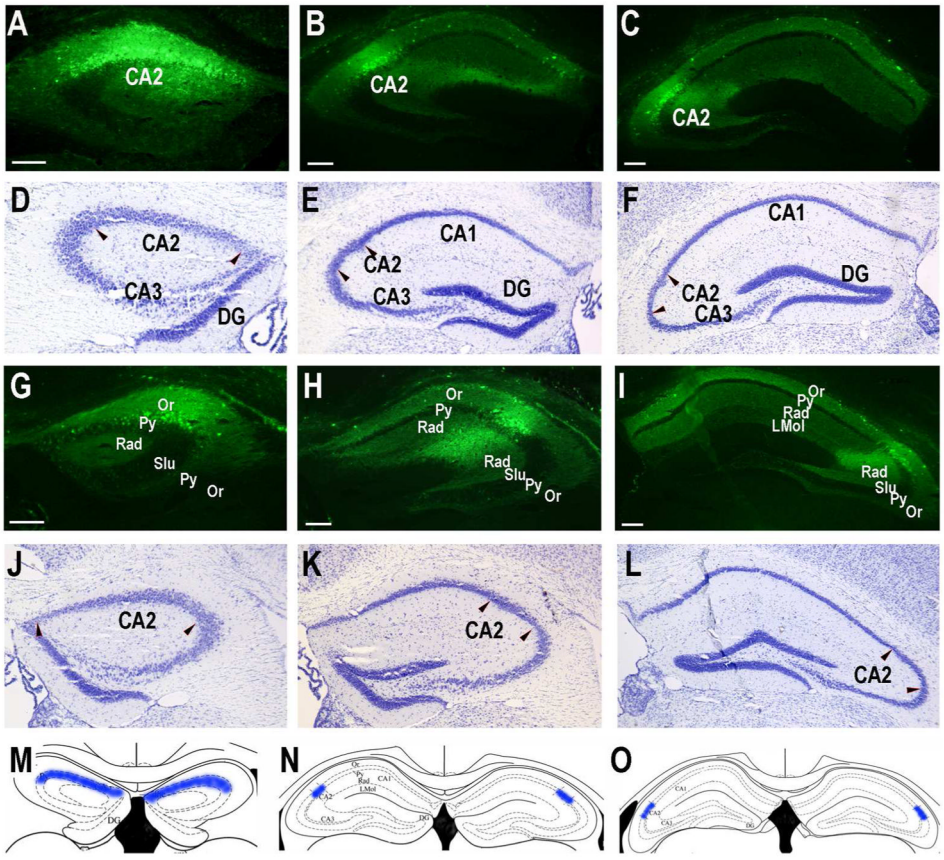

Fig. 10.

Three pairs of bilateral injections (400 nl each) of AAV-GFP to provide a comprehensive picture of dorsal CA2 efferent projections. A. Injection site: −1.25, −1.22, −1.73mm. B. Injection site: −2.00, −1.70, −1.83mm. C. Injection site: −2.60, −2.18, −2.15mm. D – F. Nissl staining of the same or adjacent sections to indicate the AAV-GFP injection sites at CA2 regions. Pairs of arrowheads delineate the CA2 boundaries. G. Injection site: 1.25, −1.22, −1.73mm. H. Injection site: 2.00, −1.70, −1.83mm. I. Injection site: 2.60, −2.18, −2.15mm. Fibers are seen in strata oriens and radiatum of CA1, CA2, and CA3 in all dorsal levels, as well as stratum lacunosum moleculare in CA1. J – L. Nissl staining of the same or adjacent sections to indicate the AAV-GFP injection sites at CA2 regions. Pairs of arrowheads delineate the CA2 boundaries. M - O. Schematics (modified from (Franklin and Paxinos, 2007) with permission) of hippocampal coronal sections representing the relative locations and structural features of hippocampal CA2 regions at panels of A & G, B & H and C & I, respectively. The shading represents the CA2 regions. Scale bars equal 100 μm (for each Nissl section, use the scale bar in the panel above).

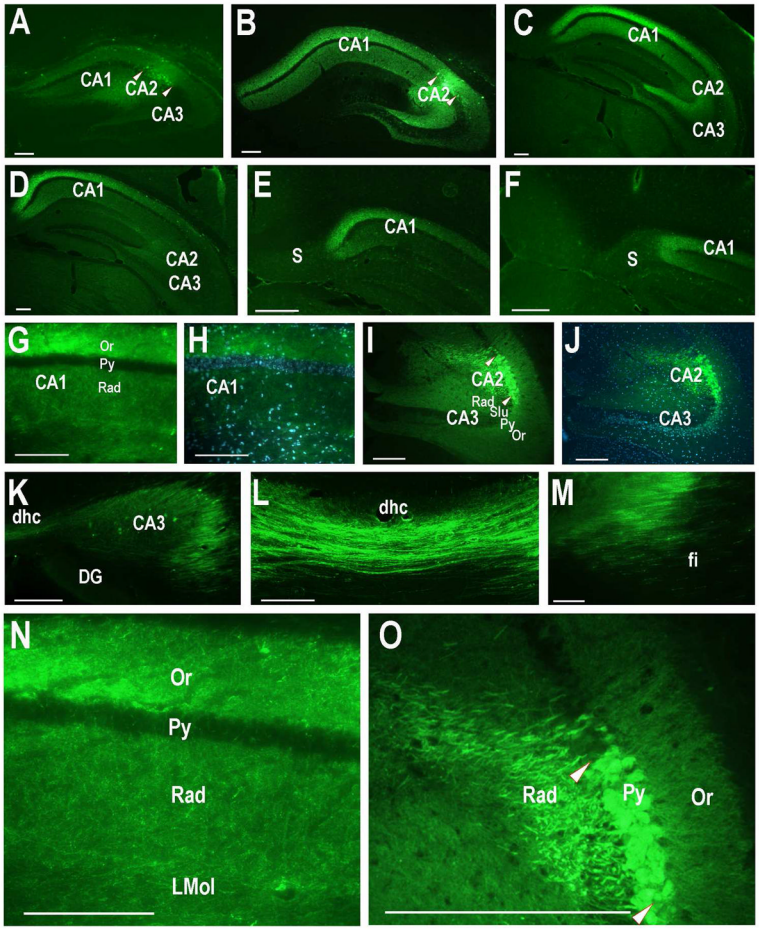

Fig. 11.

Intrahippocampal projections of dorsal CA2 neurons following six-site injections (as shown in Fig. 10). A. Fiber labeling near the CA2 injection of Fig. 10H. B. Fiber labeling near the CA2 injection of Fig. 10I. C. Fiber labeling just posterior to the CA2 injection of Fig. 10C. D. Further posterior than 11C, only dorsal aspects display fluorescence, but at a slightly reduced level. E, F. Further posterior than 11D, no fibers are labeled in the subiculum or overlying cortex and only the dorsal tip of CA1 shows GFP-positive fibers. G, H. Higher magnification of GFP-positive fibers in CA1 showing label greatest in stratum oriens and least in pyramidal cell layer. DAPI staining in H reveals cell bodies. I,J. CA2 injection site showing prominent labeled initial axons entering CA2 stratum radiatum and, to a lesser extent, into CA2 stratum oriens and the just adjacent CA3 pyramidal cell layer. Diffuse labeling is seen in CA3 strata oriens and radiatum. DAPI staining in J reveals cell bodies. K. GFP-positive fibers in the dorsal hippocampal commissure and CA3 anterior to the CA2 site 1 injection. L. GFP-positive axons traversing the dorsal hippocampal commissure. M. GFP-positive axons within the dorsal fimbria. N. Higher magnification than in panel G of CA1 region showing greater amounts of GFP-positive fibers in the stratum oriens than other layers. O. Higher magnification than in panel I showing prominent labeled initial axons entering CA2 stratum radiatum. Arrowheads delineate the CA2 regions of AAV-GFP injections. Scale bars equal 100 μm.

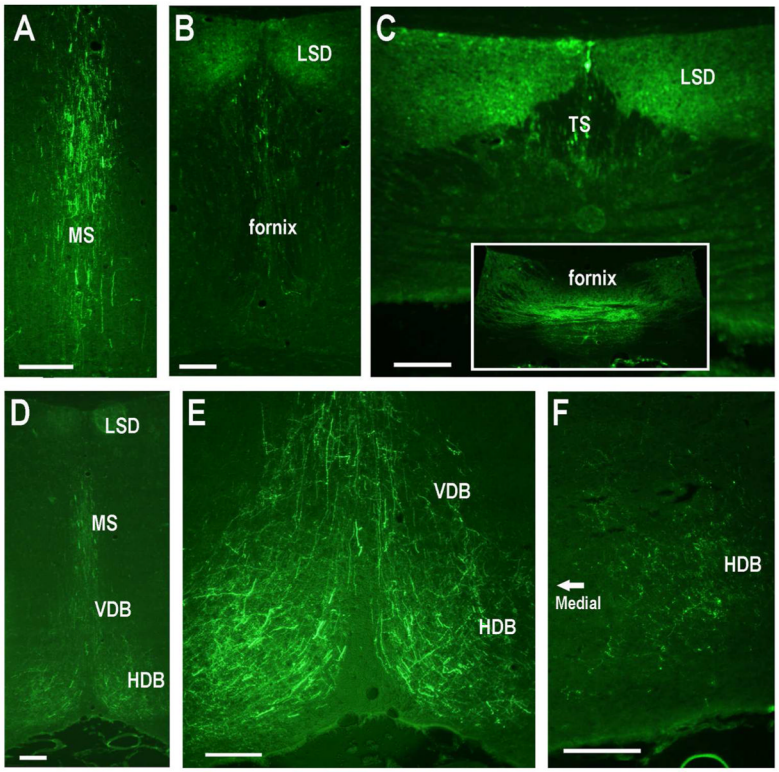

Fig. 12.

Subcortical projections of dorsal CA2 neurons following six-site injections (as shown in Fig. 10). A–C. Progressively further posterior sections showing GFP-positive fibers within the MS and then LSD, TS and fornix. D-F. GFP-positive fibers within diagonal bands of Broca. Scale bars equal 100 μm.

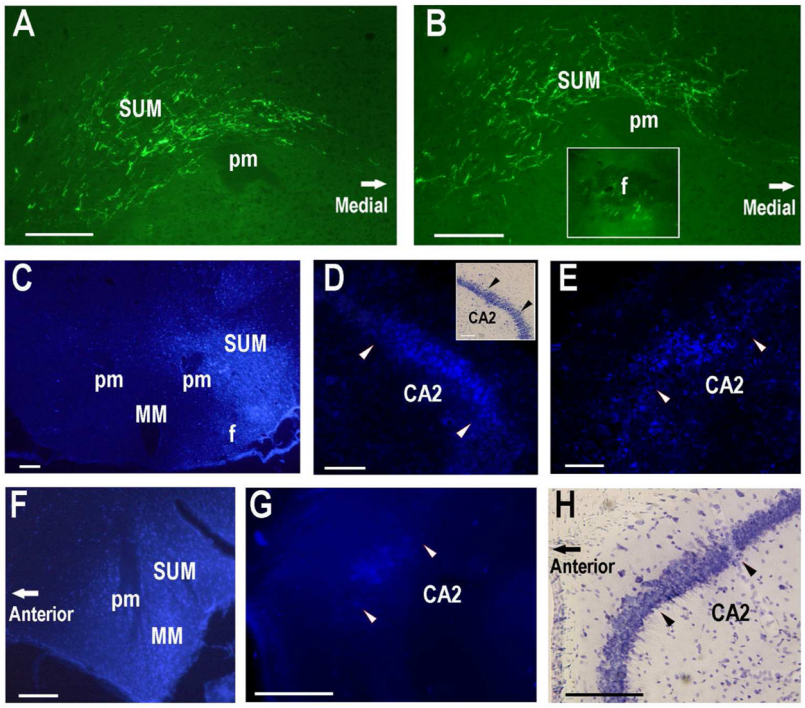

Fig. 13.

CA2 neurons send subcortical efferent projections to the supramammillary nucleus. A. Heavily labeled GFP-positive axonal fibers are present in the SUM. Only one side of SUM is shown (after CA2 injections shown in Fig. 10). B. Heavily labeled GFP-positive axonal fibers present in the more posterior SUM. The insert shows labeled fibers in the ipsiateral fornix anterior to the SUM. C. Unilateral fluorogold injection (50nl of 1%) into the SUM. D. Fluorogold labeled neurons in the ipsilateral CA2 two weeks following the SUM injection. Insert in panel D shows the Nissl staining of the adjacent section. E. Fluorogold labeled neurons in the contralateral CA2 two weeks following the SUM injection. F. Unilateral fluorogold injection (50nl of 1%) into the SUM of another mouse shown in a sagittal section. G. Fluorogold labeled neurons in the ispsilateral CA2 two weeks following the SUM injection (sagittal section). H. Nissl staining of the adjacent section. Pairs of arrowheads delineate the CA2. Scale bars equal 100 μm.